Renewable and Sustainable Energy Reviews 19 (2013) 136–163

Contents lists available at SciVerse ScienceDirect

Renewable and Sustainable Energy Reviews

journal homepage: www.elsevier.com/locate/rser

Solar assisted sea water desalination: A review

Chennan Li, Yogi Goswami*, Elias Stefanakos

Clean Energy Research Center, College of Engineering, ENB 118, University of South Florida, 4202 E. Fowler Avenue, Tampa, FL 33620, USA

ARTICLE INFO

Article history:
Received 30 January 2012
Accepted 1 April 2012
Available online 7 December 2012

Keywords:
Desalination
Energy consumption
Solar energy
Low grade heat
Cogeneration

ABSTRACT

Seawater desalination is an important process to meet the increasing demand for fresh water demand; however, it is highly energy intensive due to the high salinity of the source. Studies on using solar energy to drive seawater desalination are very actively being pursued. This paper reviews the current solar desalination research activities first, followed by discussions of solar assisted desalination processes and a variety of possible combinations. Solar assisted desalination has been proved technically feasible; however the combined solar and fossil fuel desalination, and desalination using low grade waste heat could be more cost effective at this time. Though solar assisted desalination processes have not been commercialized as yet, with the current ongoing research, they remain a valid option for future desalination plants.

Published by Elsevier Ltd.

Contents

* Corresponding author. Tel.: +1 813 974 0956; fax: +1 813 974 5250.
E-mail address: goswami@usf.edu (Y. Goswami).

1364-0321/$ - see front matter Published by Elsevier Ltd.
http://dx.doi.org/10.1016/j.rser.2012.04.059

1. Introduction

Historically, seawater desalination has been the most expensive way to produce drinking water at the commercial scale because of the high capital and energy costs [1–3]. However, desalination is increasingly recognized as a needed and viable option due to the rapid increase of the world population [4]. It is projected that close to 70% of the world population will face water shortage issues by 2025 [5–7] and approximately 50% of the world's population lives within 200 km of the coast. Since the first commercial scale desalination plant was used during World War II, the world total contracted desalination capacity, as shown in Fig. 1·[8], has grown to 71.7 million m^3/day in 2010. From Fig. 2·[8] it can be seen that seawater desalination has undergone major market expansion of the market since 2003. It is estimated that about 8.78 million tons of oil per year is required to produce by desalination 1 million/m^3/ day of fresh water [9], which indicates the importance of finding suitable alternative energy resources for the desalination systems.

Among all the alternative energy resources, solar energy is at the top of all the sources for its potential to provide for the future energy needs. Apart from providing some useful data for comparison among the resources, Table 1 illustrates that the comparison is not always simple due to different calculation methods, standards or assumptions in various studies in the literature. Many developing countries, which normally could not afford to use desalinated water, are likely to have much large needs of water due to population growth. These countries, in general, have higher solar radiation also. For example, the average daily solar radiation in India is 4–7 kW h/m^2 [10] compared with the global average of 2.5 kW h/m^2. Therefore, solar energy driven/assisted desalination is becoming more viable despite its high capital cost.

2. Solar assisted seawater desalination process

Seawater desalination may be classified by the intended product as well as the process, as shown in Fig. 3. The processes further grouped by those that allow water to pass through a membrane without phase change such as reverse osmosis (RO) and forward osmosis (FO), or processes that involve a phase change such as multi-stage flash (MSF), multi-effect distillation (MED), solar still (ST), humidification–dehumidification (HDH), passive vacuum desalination (PVD), membrane distillation (MD), freezing–melting (FM) as well as heat pump desalination applications including thermal vapor compressor (TVC), mechanical vapor compressor (MVC), absorption heat pump desalination (ABHP) and adsorption heat pump desalination (ADHP). Processes for extracting salt such as electro-dialysis (ED), ion exchange (IE) and capacitive deionization (CDI) are normally used in brackish water desalination but not seawater desalination. Among all of the above mentioned desalination processes, MSF, MED, RO and ED account for about 95% of the global desalination capacity, as can be seen in Fig. 4·[8].

2.1. Solar assisted MSF

Multi-stage flash has the second largest installed desalination capacity after the RO systems. Most of the energy consumption of MSF is the thermal energy used to distill water, while some electricity is needed for pumping. As can be seen in Fig. 5, MSF could be connected with a solar thermal heat source and the power grid at the same time, or it could be connected with a solar thermal system through a heat engine to provide heat and electricity at the same time. A solar pond type of solar thermal system may be especially applicable, since the produced salt could be used in the pond itself.

In a MSF process, seawater moves through a sequence of vacuumed reactors called stages that are held at successively lower pressures where seawater is preheated. External heat is supplied to heat the preheated seawater above its saturation temperature. Seawater is then successively passed from one stage to the next in which a small amount of water flashes to steam in each stage and the remaining brine flows to the next stage for further flashing. The flashed steam is condensed and collected as fresh water after removing the latent heat of condensation to preheat the entering seawater at each stage. MSF is used in large scale cogeneration power plants [14–18] because it can use low-quality steam rejected from power cycles as the heat source. Some researchers claim that MSF is not as thermally efficient as MED [19] while others do not see any clear advantages in the thermodynamics of the MED process over the MSF process other than the thermal losses that are higher in the MSF than in the MED due to its higher operating temperature [20].

2.1.1. Solar pond driven MSF

A solar pond (SP) is a stable pool of salt water in which the water salinity increases in the middle layer from its top to the bottom with a gradient that prevents convective mixing on absorbing solar radiation and the resulting increase in temperature, as shown in Fig. 5. Heat is passively collected and stored in the lower convective zone (LCZ) because the middle layer is a non-convective zone (NCZ).

Most commercial MSF units operate with a top brine temperature of 90–110 °C [21] heated by steam while the solar pond operates in the range of 30–95 °C. Therefore, in solar pond assisted MSF systems, the first stage of the MSF heat exchangers is changed to a liquid–liquid heat exchanger instead of steam–liquid heat exchanger [22]. Some selected solar pond assisted MSF research studies are listed in Table 2.

Due to the intermittence of solar radiation, conventional MSF with fixed orifices and weirs to control inter-stage pressures are not suited for these abrupt changes of pressure differences between stages. Atlantis "*Autoflash*" MSF [23] used a proprietary passive inter-stage pressure regulation system that could be self-regulating at each fluid passage between the stages. Since a solar pond is a solar collector and storage in one, it overcomes the intermittent nature of solar energy. However, the solar pond has to be oversized for winter conditions, necessitating some of the surplus summer heat to be wasted [26]. On the other hand, waste heat from other sources (gas turbine, for example) may be used during periods of insufficient sunshine [29]. These kinds of hybrid solar pond systems could store extra waste heat, such as from gas turbine exhaust during peak times to lower the water production cost and the solar pond size [25]. Table 2 shows that a hybrid system using low grade heat has a relatively lower water cost.

Nomenclature

W_{SWRO}	Work required for seawater RO system [kJ]
h_s	specific enthalpy of feed seawater [kJ/kg]
w_{min}	minimum work required [kJ]
Q_{input}	Heat input [kJ]
g	specific Gibbs energy
Q_{loss}	Heat loss to the environment [kJ]
α	recovery
q_s	specific energy consumption [kg/kg]
V_{fresh}	the produced fresh water volume
m_f	sum of the mass of the final fresh water production
η_{pump}	pump efficiency
m_{fv}	fresh water vapor mass
ΔP	overpressure above the osmotic pressure [k Pa]
λ	latent heat at the final product temperature
η_{ERD}	efficiency of ERD
E_d	exergy destruction
R	gas constant
ΔS	entropy change
P_{sea}	osmotic pressure [kPa]
h_{fl}	specific enthalpy of fresh water vapor [kJ/kg]
h_b	specific enthalpy of concentrated brine [kJ/kg]

Subscripts

T_0	environmental temperature
br	rejected brine
ΔX	generalized driving force conjugated to the flow $\Im$
w	produced fresh water
$\Im$	flow rates
w	feed seawater

Abbreviations

RO	reverse osmosis
HDH	humidification–dehumidification
FO	forward osmosis
PVD	passive vacuum desalination
MSF	multi-stage flash
MD	membrane distillation
MED	multi-effect distillation
FM	freezing–melting
ST	solar still
TVC	thermal vapor compressor
MVC	mechanical vapor compressor
ABHP	absorption heat pump desalination
ADHP	adsorption heat pump desalination
ED	electro-dialysis
IE	ion exchange
CDI	capacitive deionization
SP	solar pond
LCZ	lower convective zone
NCZ	non-convective zone
GOR	gained output ratio
UCZ	upper convective zone
PV	photovoltaic
ETC	evacuated tube solar collectors
HP	Heat Pump
ORC	organic Rankine cycle
CAOW	closed air, open water
CWOA	closed-water open-air
DCMD	direct contact membrane distillation
AGMD	air gap membrane distillation
SGMD	sweeping gas membrane distillation
VMD	vacuum membrane distillation
FPC	flat panel collectors
DEAHP	double absorption heat pump
TES	thermal energy storage
CPC	compound parabolic collector
PTC	parabolic trough collectors
CSP	concentrating solar power
EDR	energy recovery device
ppm	parts per million

Solar ponds have many advantages over other solar desalination technologies [30], such as low cost per unit area of the collector, inherent storage capacity and capability of utilizing reject brine, which is often considered as a waste product for other processes [31]. In addition, the solar pond surface water could be used as cooling water because of its lower temperature during the summer months [27]. However, solar ponds need sunny conditions, large flat land and might have environmental impacts such as soil contamination by pond brine leakage [29,32], etc. In addition, the solar pond salinity profile needs to be carefully

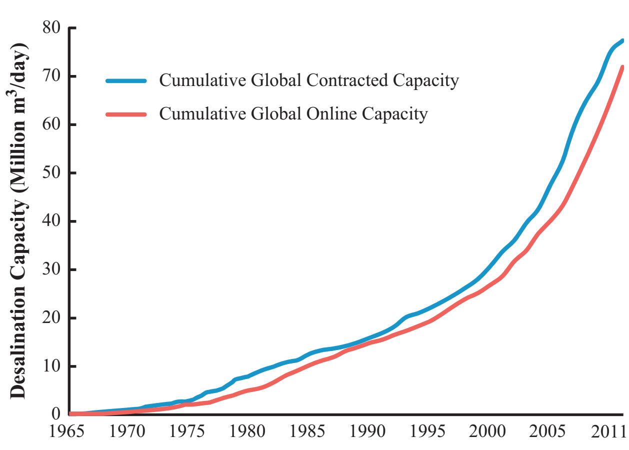

Fig. 1. Total contracted commissioned desalination capacity, 1965–2010 [8].

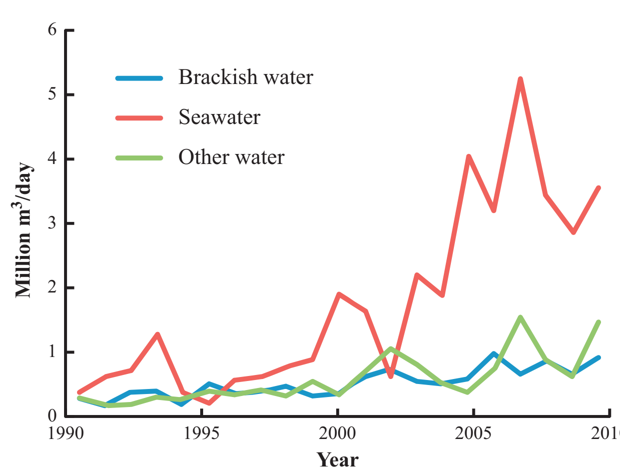

Fig. 2. Annual new contracted desalination capacities by feed water, 1990–2010 [8].

Table 1
Worldwide technical potential energy, installed capacity, current economic potential and capacity factor [a].

Types of technology	Technical potential (TW)			Installed capacity (GW)	Installed capacity (GW)	Current economic potential (TW)	Worldwide capacity factor of technology in place
Solar							
PV	342.26[b]	60[c]	> 50[d]	8.7[b]	5[c]	0.15–7.3[c]	0.1–0.2[b]
CSP	0.89[b]			0.354[b]			0.13–0.25[b]
Others	NA			NA			NA
Wind	46.77[b]	2[c]	20[d]	94.1[b]	6[c]	0.6[c]	0.205–0.42[b]
Geothermal	0.14[b]	11.6[c]	3.8[d]	9[b]	54[c]	0.6[c]	0.73[b]
Hydroelectric	1.88[b]	1.6[c]	1.6[d]	778[b]	650[c]	0.8[c]	0.416[b]
Wave	0.50[b]	NA	NA	0.00075[b]	NA	NA	0.21–0.25[b]
Tidal	0.02[b]	NA	NA	0.26[b]	NA	NA	0.2–0.35[b]
Nuclear	13.92[b]	NA	NA	371[b]	NA	NA	0.808[b]
Coal-ccs	1.25[b]	NA	NA	NA	NA	NA	0.65–0.85[b]
	NA	6–8[c]	9[d]	NA	1600[c]	NA	NA

[a] For comparison, the 2005 world electric power production was 2.08 TW; the energy production for all purposes was 15.18 TW.
[b] Data from Ref. [11].
[c] Data from Ref. [12].
[d] Data from Ref. [13].

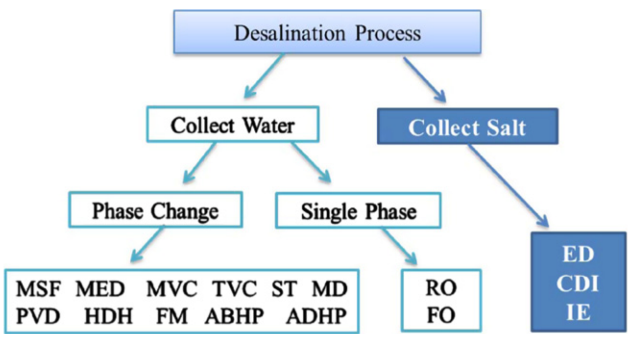

Fig. 3. Desalination process grouped based on which substance is extracted.

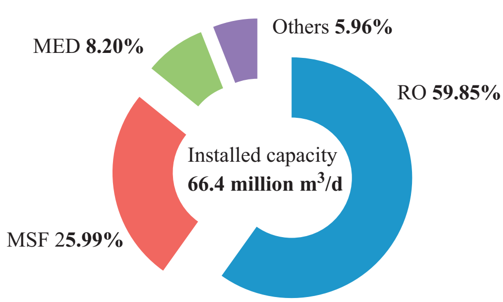

Fig.4. Total worldwide installed desalination capacities by technology, 2010 [8].

maintained, the saline water needs to be kept at low pH, the pond clarity needs to be monitored very carefully, and the wind factor needs to be considered before the construction.

2.1.2. *Solar collector driven MSF*

Some researchers claim that it is better to use indirect solar desalination for large desalination projects [33], which means that a solar collector field is connected with a conventional distillation plant to provide thermal energy for the desalination process. Solar collectors can be classified as concentrating and non-concentrating types. Table 3 shows different thermal collectors and their operating temperatures [34]. Solar collectors are chosen based on the desired process temperature. Concentrating solar systems can be trough, dish or central receiver tower types. One of the main advantages of concentrating solar systems over most other renewable electricity technologies is that they can be operated in conjunction with large heat storage facilities (e.g., using molten salt or concrete) or in hybrid mode with fossil fuel or biomass, to compensate for the fluctuations in daily irradiance and to produce electricity beyond the sunshine hours [35].

Some selected solar collector assisted MSF seawater desalination systems are seen in Table 4. Hou et al. [36] used pinch analysis to optimize a solar multi-stage flash (MSF) desalination process and concluded that, in order to enhance the performance, a wide working temperature range of MSF is needed, and, in order to gain higher gained output ratio (abbreviated as GOR, and defined as the number of kilograms of desalinated water produced per kilogram of steam consumed), it is better to discharge the brine at the last stage. It was found that controlling the flash evaporation pressure is important, i.e., by reducing the flash evaporation pressure from 0.014 MPa to 0.010 MPa, the desalination rate could increase almost 5 times in some direct solar thermal desalination systems [39].

In general, MSF series connected stages require precise pressure and temperature control and some transient time is needed to establish the normal running operation of the plant. Since the solar heat source is intermittent, an effective thermal storage system, i.e., a storage tank, can be used for thermal buffering [44]. MSF uses the seawater feed as the coolant which means that MSF uses sensible heat to recover the latent heat from the distilled water. Therefore MSF requires large amounts of seawater recirculating within the system and consumes more electricity than a MED process.

2.2. *Solar assisted multiple effect distillation (MED)*

Similar to the solar assisted MSF process, the solar assisted MED process also needs both thermal energy and mechanical energy. MED may be operated in three configurations: forward feed, backward feed and parallel feed. Fig. 6 shows the schematic of one solar assisted parallel feed MED, in which seawater is delivered to a sequence of successively low pressure vessels, called effects. The external heat is supplied to the first effect and the generated vapor of the previous effect supplies its latent heat of condensation to the next effect.

Unlike MSF which recovers latent heat of the vapor by the sensible heating of the seawater, MED systems reuse latent heat vaporizes the seawater. The specific heat capacity of water is approximately 4 kJ/kg/K while the latent heat of vaporization is approximately 2300 kJ/kg, therefore MED systems normally have 2–14 effects while MSF systems have more than 20 stages. MED systems use falling film horizontal tube evaporator/condensers for high heat transfer efficiency [45,46]; operate with a relatively

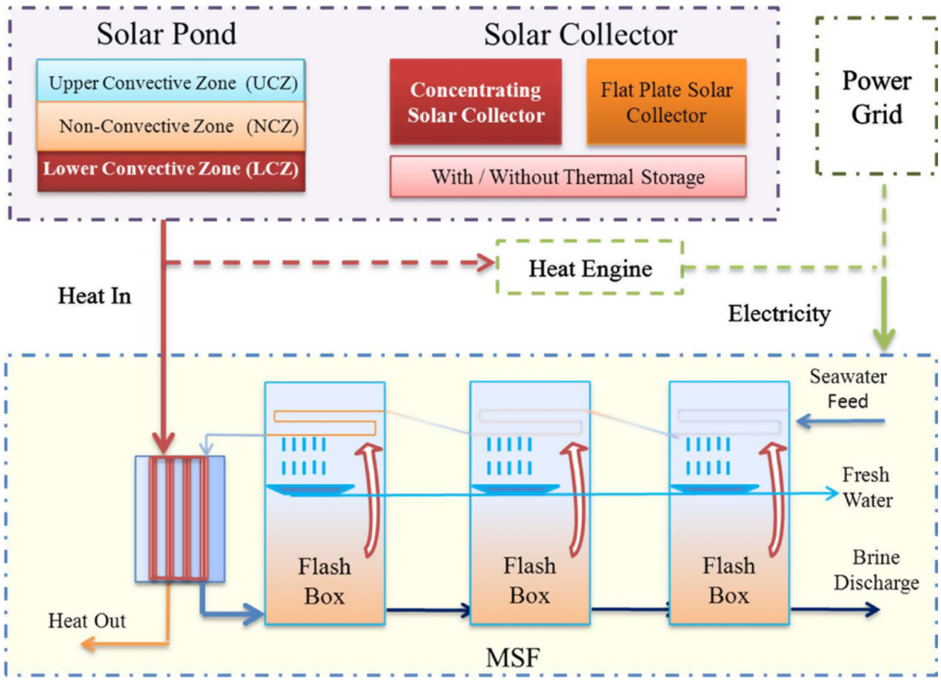

Fig. 5. Schematic of solar assisted multi-stage flash desalination process.

Table 2
Selected solar pond assisted MSF research.

Refs.	Mod/ exp.	Location/ radiation	Pond size (m^2)	Top brine temp. (°C)	Capacity (m^3/d)	Cost ($/$m^3$)	GOR	*N.* of stages	Desal cost perc.	SP cost perc.	Notes
[23]	Model	North Africa[a]	2500	< 95	15	5.48	NA	12–14	0.728	0.272	[h]
			36000		300	2.39	NA		0.745	0.255	
[24]	Exp.	Qatar	1500	55–80	20	NA	NA	22	NA	NA	
	Model	5.5–6 kW h/m^2/d	80000		1000	2.85	NA	NA	0.267[b]	0.18[b]	
			800000		10000	1.84	NA	NA	0.251[b]	0.174[b]	
[25]	Model	4.54 kW h/m^2/d[m]	7800	< 75, 95–120[o]	2040[m]	0.916[p]	9.2–12.5	NA	NA	NA	Hybrid
					12378[n]	0.827[p]	10.4–13.5				
[26]	Model	Tripoli, Libya[e]	70000	< 90[d]	1570[g]	1.8[f]	10[i]	31[j]	NA	NA	[k]
[27]	Mod/ exp.	El Paso, US	3000	57–77	1.6–9	NA	3.2–6.2	24	NA	NA	[l]
[22]	Model	246.3 W/m^2	65361	88	550	3.71	6	20	0.343[c]	0.590[c]	[m]
			49441			3.42	8		0.431[c]	0.502[c]	
[28]	Model	Safat, Kuwait[q]	NA	< 78	1	1.785[q]	[r]	18	NA	NA	Hybrid
				< 78	1	2.835[q]					Solar

[a] Author mentioned North Africa and if location is Tripoli, Libya, NASA data showed 5.11, 6.03 kW h/m^2/d for annual average global radiation and DNI average radiation.
[b] Interests, which are 7% for 15years, are not included.
[c] O&M cost is not considered.
[d] Solar pond temperature ranges 65–106 °C.
[e] Figures from the paper showed that radiation less than 350 W/m^2, NASA data showed location has monthly average radiation 5.11 and 6.03 kW h/m^2/d for horizontal and DNI.
[f] The minimum break even fuel cost was $209.261/ton occurred when the lower convective zone of the solar pond temperature is 90 °C and a desalination process performance ratio of 8 with an interest rate of 6%, cost varies 1.8–1.94 depend on MSF GOR and pond *T*.
[g] Capacity varies 1238–1570 m^3/d based on solar pond temperature.
[h] Auto flash: a desalination unit which is capable to operate smoothly under variable input conditions. An inter-stage pressure regulation device was incorporated at each fluid passage (brine and distillate) to replace the conventional orifices between the stages.
[i] GOR 4–10 based on maximum solar pond temperature 90 °C.
[j] Stages vary 14–31 based on solar pond *T*, when GOR is 10 the relative MSF has 28 stages heat recovery and 3 stages heat rejection.
[k] About 73–185 m^2/m^3/d capacity depending on the storage zone temperature, peak clipping days and the performance ratio.
[l] Falling film spin flash unit.
[m] Main heat source is exhaust gas from a 30 MW gas turbine 550 °C. Part of the heat is used to run a desalination plant and the rest is stored in a solar pond (depth 4 m). Radiation data same with (l).
[n] Main heat source is exhaust gas from a 120 MW gas turbine, rest conditions are the same as [k]. Based on authors proposed location, south of Tunisia, NASA data showed horizontal monthly annual average at horizontal 4.54 kW h/m^2/d and direct norm radiation 5.24 kW h/m^2/d.
[o] Peak time heated by gas turbine, seawater temperature 95–120 °C while rest of the time by solar pond, 75 °C.
[p] The surface pond is covered by a transparent material to reduce heat losses and store solar energy. Price range 09–0.1014 for gas turbine and solar pond driven separately, average cost 0.916; Price range 0.821–0.862 for gas turbine and solar pond driven separately, average 0.827.
[q] Convert to dollar based on 1 KD=3.5 dollar as authors mentioned, based on author mentioned location, NASA data showed 5.4, 6.33 kW h/m^2 for monthly average horizontal and DNI radiation.
[r] Thermal energy input, 167 kJ/kg; electricity energy input, 25 kJ/kg.

Table 3
Solar collectors and their characteristics [34].

Tracking	Collector Type	Absorber	Concen. ratio	Operational range (°C)
Stationary	Flat plate (FPC)	Flat	1	30–80
	Evacuated tube (ETC)	Flat	1	50–200
	Compound parabolic (CPC)	Tubular	1–5	60–240
Single-axis	Compound parabolic	Tubular	5–15	60–300
	Linear Fresnel	Tubular	10–40	60–250
	Parabolic trough (PTC)	Tubular	15–45	60–300
	Cylindrical trough	Tubular	10–50	60–300
Double-axis	Parabolic dish	Point	100–1000	100–500C
	Heliostat field	Point	100–1500	150–2000

Table 4
Some selected solar collector assisted MSF seawater desalination systems.

Refs.	Mod/exp.	Location	Capacity (m^3/d)	Collector type	Collector size (m^2)	Cost ($/$m^3$)	N of stages	Top Brine T (°C)	Global radiation (kW h/m^2/d)[a]	DNI (kW h/m^2/d)[a]
[37,38]	Model	PSA, Spain[b]	1200–3000[b]	PTC[b]	41880[b]	2.5–4	24[b]	<105	4.65	5.6
[39]	Exp.	Tianjin, China	0.3	Flat	NA	4.67	1[c]	78	4.36	5.58
			6	Flat	NA	3.9		78	4.36	5.58
[40]	Exp.	Gaza[d]	0.145	Flat	5.1	NA	3	NA	5.57	6.98
[41]	Model	Benghazi, Libya	8.3	Flat	1[e]	NA	NA	80	5.44	6.76
			13.2	CPC	1[e]	NA	NA	122		
[42]	Exp.	Tamilnadu, India[f]	0.0085[f]	Flat	2	9	1	NA	5.22	4.97
[43]	Mod/exp	Suez, Egypt[g]	0.0025–0.0165	Flat	2.39	NA	1[g]	40–67	5.69	7.03

[a] Data based on locations author mentioned from NASA Surface meteorology and Solar Energy; Global Solar Radiation is defined as the amount of electromagnetic energy (solar radiation) incident on the surface of the earth, also referred as total or global solar radiation. The average and percent difference minimum and maximum are given. Direct normal radiation (DNI) is defined as the amount of electromagnetic energy (solar radiation) at the Earth's surface on a flat surface perpendicular to the Sun's beam with surrounding sky radiation blocked.

[b] MSF GOR = 10, capacity 100 m^3/h; 10–16 m^3 water/m^2 collector; Location: plataforma solar de Almeria, Spain; PTC is horizontal north–south collectors (Solar Kinetics T700A) with a distance of 7 m between homologous pointsinto the solar field and row azimuth equal to 0 °. Synthetic thermal fluid (Santotherm 55) with inlet/outlet temperatures of 125 °C/205 °C or lower, but above 100 °C; temperature change of the thermal oil in the solar field, about 80 °C. The system has a thermocline vessel thermal storage.

[c] Seawater first flash evaporation then use generated vapor to distill brine.

[d] Location: Al Azhar University at Gaza; Radiation range 2.83–8.19 kW h/m^2/d, June–July.

[e] Aperture area.

[f] Maximum daily production is 8.5 L/d, which is 3 times higher than a solar still at Tamilnadu, India with beam solar radiation range 400–900 W/m^2.

[g] Performance ration 0.7–0.9, solar radiation ranges 2.79–5.12 kW h/m^2/d.

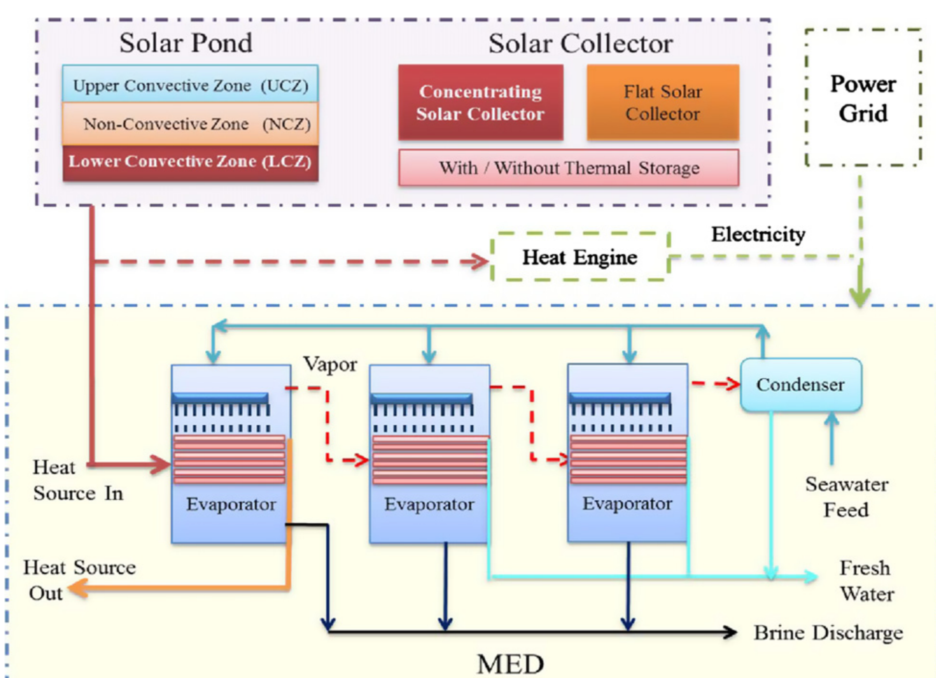

Fig. 6. Schematic of solar assisted multi-effect distillation desalination process.

low top brine temperature (usually lower than 75 °C) to reduce scale formation and corrosion [47]; and can be combined with heat pumps to improve the overall efficiency [48–50]. The combination of economic costs and low energy consumption, together with the inherent durability of the low temperature MED, avoid the necessity of comprehensive sea water pretreatment (such as with RO plants) and make the MED process one of the best candidates for safe and durable large capacity desalination [51]. Compared to MSF, MED has high overall efficiency, high heat transfer co-efficient, relative independent stages and less water recycling [52]. However, in order to lower the energy consumption, MED needs large surface area of evaporators to reduce the temperature difference of adjacent stages; and, some research has shown that when operating with high-pressure steam, MED consumed more energy than MSF [20].

2.2.1. Solar pond assisted MED

A solar pond assisted MED system is similar to a solar pond driven MSF system. However, lower temperature need of MED makes the solar pond operation relatively easier. By mathematical modeling, Hawaj and Darwish[53]found that intermediate steam supply temperatures (80–90 °C) are more efficient for the operation of solar-assisted MEB systems because higher steam supply temperatures decrease the solar enhancement; A large ratio of solar pond surface area with MED heat transfer area leads to continuous increase in pond temperature [53]; Garman and Muntasser found that [54] the optimum thicknesses for upper convective zone (UCZ), non-convective zone (NCZ) and lower convective zone (LCZ) were reported as 0.3 m, 1.1 m and 4 m, respectively, for low temperature MED systems. Some selected solar pond assisted MED systems are listed in Table 5, also includes a special multi-effect, multi-stage distillation (MEMS) which is a combination of MSF and MED systems [27,55]. Table 5 also shows that hybrid systems, similar to the solar pond assisted MSF plants, have lower unit water cost.

2.2.2. Solar collector assisted MED

Solar collector assisted MED seawater desalination processes have been studied extensively. Table 6 shows some selected solar collector assisted MED systems. Some solar MED systems were combined with heat pumps to improve their performance. Based on long-term tests, the technical feasibility and reliability of solar collector assisted MED have been proved. Two long term experimental units are the Abu Dhabi solar desalination plant and the Solar Thermal Desalination (STD) Project at the Platform a Solar de Almeria (PSA), Spain.

The Abu Dhabi solar desalination plant, operated from 1984 to 2002, used evacuated tube solar collectors (ETC) assisted MED systems [62]. Researchers developed a simulation program "SOLDES" [63] to predict the part load performance [64], optimize the operating parameters so as to maximize the evaporator distillate production for every month of the year [65]. Some plant maintenance were needed, for example, dust deposition could cause the water production to drop to 40% of the clean collector production [66]. The economic feasibility studies [67,68] showed that it is not worth operating the desalination system solely on solar energy due to the high percentage of inactive time [69]. When electricity cost is above \$0.071/kW h in Israel [70], the solar-MED plant is more economical than RO.

The Spain PSA site used a 14 stage forward feed MED system with a capacity of 3 m^3/h [71]. The project had two phases. Phase I was to study the reliability and technical feasibility of a solar thermal technology application to seawater desalination which used PTC with 14 stage MED. Phase II used a double absorption heat pump to improve the system performance as shown in the next section.

2.3. Solar assisted heat pump (HP) desalination

HP units are generally used for small or medium scale [72,73] applications and they are normally combined other thermal

Table 5
Some selected solar pond assisted MED seawater desalination systems.

Refs.	Model/exp.	Location/radiation	Pond size (m^2)	Top brine *T* (°C)	Desal cap. (m^3/d)	Cost (\$/m^3)	*N.* of sages
[56]	Model[a]	Athens	30,000	< 75	500	2	14
[57,58]	Experiment	U. of Ancona (Italy).	625	< 65	30	3.66[d]	4
[27,55]	Model/exp.	5.7 kW h/m^2/d[f]	3,000	63–80	2.3–7.2[c]	0.52–0.62[e]	4[b]
[59]	Experiment	Bundoora, Australia	720	< 85[g]	0.9–2.3	18–22	3
	Model		11,800		50–130	3.4–5.1	12
	Model		58,900		260–650	1.7–3.4	12
[60]	Model	2000 kW h/m^2/y[h]	1,200,000	55	20000	0.89	(i)
			12,000,000		200000	0.71	(i)
			600,000		20000	0.79	Hybrid[j]
			6,000,000		200000	0.65	Hybrid[j]
[61]	Model	2400 kW h/m^2/y	3,300,000–4,200,000	72	100000	0.67–1.44	12
[25]	Model	4.54 kW h/m^2/d[k]	7,800	< 75, 95–120[m]	2348	0.618–0.64	30, Hybrid
		4.54 Wh/m^2/d[l]			15044	0.465–0.471	

[i]MED operates with 6.5–7.5 kW h/m^3 (including 1.5–20 kW h/m^3 for pumping and other auxiliaries).
[a] It is assumed that the combined system begins operation in spring at day N=100 when brine and soil are isothermal.
[b] Multi-effect, multi-stage flash distillation. The MEMS unit is a three effect, four stage system.
[c] This paper reported experimental tests showed that distilled water production 450 to 2270 L/h, 2.3–7.2 m^3/d.
[d] Reported data 2.68 Euro, used 1 Euro U.S. dollar=1.3656 U.S. Dollars.
[e] Hybrid system estimated cost, assume system used brine from 1 MGD to 10 MGD RO plant, solar pond liner cost is \$4/m^2.
[f] Location is El Paso, the annual average irradiation data is 5.7 kW h/m^2/d.
[g] Solar pond supply temperature 50–85 °C.
[h] Annual total insolation; Based on authors mentioned location, NASA data showed annual daily radiation 5.72 kW h/m^2/d at horizontal, 7.43 kW h/m^2/d for direct beam radiation.
[j] MED followed by RO hybrid systems powered by solar pond that are estimated to consume 5.5–6.5 kW h/m^3.
[k] Main heat source is exhaust gas from a 30 MW gas turbine 550 °C. Part of the heat is used directly to run a desalination plant and the rest is stored in a solar pond (depth 4 m). Radiation data same with (l).
[l] Hybrid plants. Main heat source is exhaust gas from a 120 MW gas turbine, rest conditions are the same as (k). Based on authors proposed location, south of Tunisia, NASA data showed horizontal monthly annual average at horizontal 4.54 kW h/m^2/d and direct norm radiation 5.24 kW h/m^2/d.
[m] Peak time heated by gas turbine, seawater temperature 95–120 °C while rest of the time by solar pond, 75 °C, MED GOR is 21.5.

Table 6
Selected Solar Assisted MED Systems.

Ref.	Mod/exp	Location/radiation	Global radiation	DNI	Cost	Capacity	Collector	N of stages	Operation temperature	Collector area	Notes
[79]	Model	Richmond, California	4.57[j]	5.54[j]	2.05–4.7	0.151	FPC/EPC	7–12	< 95	NA	
[70]	Model	Eilat, Israel[i]	5.65	6.91	0.92	10,000	PTC	16	NA	NA	
		Zikim, Israel[h]	5.57	6.99	0.69	100,000				750,000–900,000	Hybrid
[80]	Model	Southern Mediterranean	2000 kW h/m^2/y; peak radiation 1000 W/m^2		2	1,000	ETC	NA	NA	NA	
[67]	Model	Abu Dhabi, UAE	5.61	6.41	8.6–9.9	100	ETC–PV	10–30	60–80	2,500–12,500	PV
					8.3–9.3	100	ETC				Diesel hybrid
					5–6.7	500					
					3.4–4.4	1,000					
[81]	Exp.	Abu Dhabi, UAE	5.81[g]	6.41	6.58–10[d]	120	ETC	18[e]	< 76.5	1862[f]	
[82]	Exp.	Sydney	4.98	5.93	4	100	FPC	NA	NA	NA	
					5.1		ETC				
[83]	Mod/exp	PSA, Spain[k]	4.65	5.6	NA	72[l]	PTC	14[l]	< 70	500	(l)

[a] \$1.1/m^3 for hybrid plant using \$0.18/kg diesel oil when solar-steam is not available. Total land area is 14,000 m^2 for solar only 1000 m^3/d plant, 1420,000 m^2 for 100,000 m^3/d plant.
[b] A combination of a large number of effects of evaporation, together with high pressure saturated steam available for recycling, increased the calculated economic ratio (ER) from 7 to 16—a factor of 2.3, while the installation expenses grew by 60%.
[c] Utilization of solar energy is assumed to be about 2500 effective hours per year, which is about 30% of the storage capacity or fossil fuel backup.
[d] Without considering others, water cost \$6.58, when considering the contribution of capital amortization representing about 85% of the total cost and only 15% contributed by operation and maintenance expenses, the total cost of water ranges from about 7 \$/m^3 to 10 \$/m^3.
[e] 18 Stages MED system, 17 preheaters, performance ratio 12.4, with 3 tanks total 300 m^3 as water heat accumulators.
[f] collector total absorber area 1862 m^2, each collector 1.75 m^2.
[g] Authors mentioned Annual mean daily solar radiation 5000 kcal/m^2/d.
[h] Southern end of Israel's Mediterranean shore, and the author gave one case study at Zikim.
[i] The author used Eilat as one typical place for area close to Israel red sea close area.
[j] Estimated from NASA data based on author location.
[k] Plataforma Solar de Almería, Spain; Phase I of the STD project considered the reliability and technical feasibility of solar thermal technology application to seawater desalination.
[l] Capacity is 3m^3/h, assume 24 h operation which is 72 m^3/d; 14 effects MED has performance ratio 9.4–10.4; vacuum generated by Hydroejectors using 3 bar seawater.

processes [74–78]. There are four basic types of heat pump applications in desalination processes [48]. These include thermal vapor compressor (TVC) (Fig. 7a), mechanical vapor compressor (MVC) (Fig. 7b), absorption heat pump (ABHP) (Fig. 7c) and adsorption heat pump (ADHP) (Fig. 7d) [49].

TVC could be used with MED or MSF in different sizes of commercial desalination plants [84–87], in which the steam compression is carried out by an ejector and the vapor from the last effect of the MED process is carried by a motive stream back to the first effect. MVC is widely studied and used because of its simplicity and relative low energy consumption [88–91]. The bottoming condenser is eliminated because the entire vapor formed in the last stage is routed to the mechanical vapor compressor, where it is compressed to the desired temperature and pressure in order to recover heat in the rejected brine and distillate product streams. ABHP [92–96] absorbs the last effect vapor through LiBr-water and discharges steam for use by the first effect; while ADHP [97,98] uses zeolite–water or other pairs to recover vapor from the last effect MED and generate high temperature steam through a desorber bed II. ABHP and ADHP are regarded to have higher potential for applications in desalination than TVC and MVC [49,99], however, at the present time there are no commercial applications.

All heat pumps combined thermal desalination systems recover the low temperature vapor from certain parts of the MED/MSF system and convert it to higher temperature vapor in order to improve the system efficiency. Furthermore, since low temperature vapor could be recovered, the whole desalination system needs less cooling water and consumes less electricity. The differences among various heat pump based systems are that (1) MVCs use electricity as energy source (Fig. 8) and could be used as stand-alone desalination systems; (2) TVCs use higher temperature and pressure (> 200 kPa) steam; (3) ABHP and ADHP use either higher temperature steam or other heat sources in the absorption/adsorption cycles. Solar assisted heat pumps combined with other desalination processes could be used as shown in Fig. 8. MVC must be driven by mechanical energy therefore a photovoltaic (PV) system or a heat engine are used; TVC/ABHP/ADHPs use steam therefore they are connected between the solar thermal process and the thermal desalination process.

Among all the research activities listed in Table 7, the project AQUASOL achieved the lowest experimental specific energy cost as listed in Table 8 [100]. The AQUASOL project is the continuation of the previous STD Project [38,101–104] mentioned in Section 2.2.2. It is composed of [105]: (i) a 14-effect MED, (ii) a 500 m^2 stationary CPC collector field, (iii) a 24 m^3 thermal storage system based on water, (iv) an advanced prototype of LiBr–H_2O double effect absorption heat pump (DEAHP), and (v) a smoke tube gas boiler to guarantee 24 h operation. Researchers found that the connection between the absorption heat pump and the MED unit should not be direct by means of a closed water circuit that is heated by the heat pump and cooled by the MED unit, but indirect, by means of two auxiliary tanks [105]. The cost could be lowered to about \$2/m^3 of distillate for large plants [106,107], which is comparable to conventional MED, but the optimization depends on the cost of fossil fuels and solar collectors [108].

2.4. Solar assisted reverse osmosis (RO)

As illustrated in Fig. 9, RO, which is the biggest desalination process internationally in terms of capacity, requires only electricity from PV or mechanical energy from a solar pond or collector through a heat engine such as a sterling engine or a Rankine engine, etc. [119]. RO requires extensive water pretreatment but is energy efficient compared to phase change thermal processes, and part of the consumed mechanical energy can be reclaimed from the rejected concentrated brine with a suitable

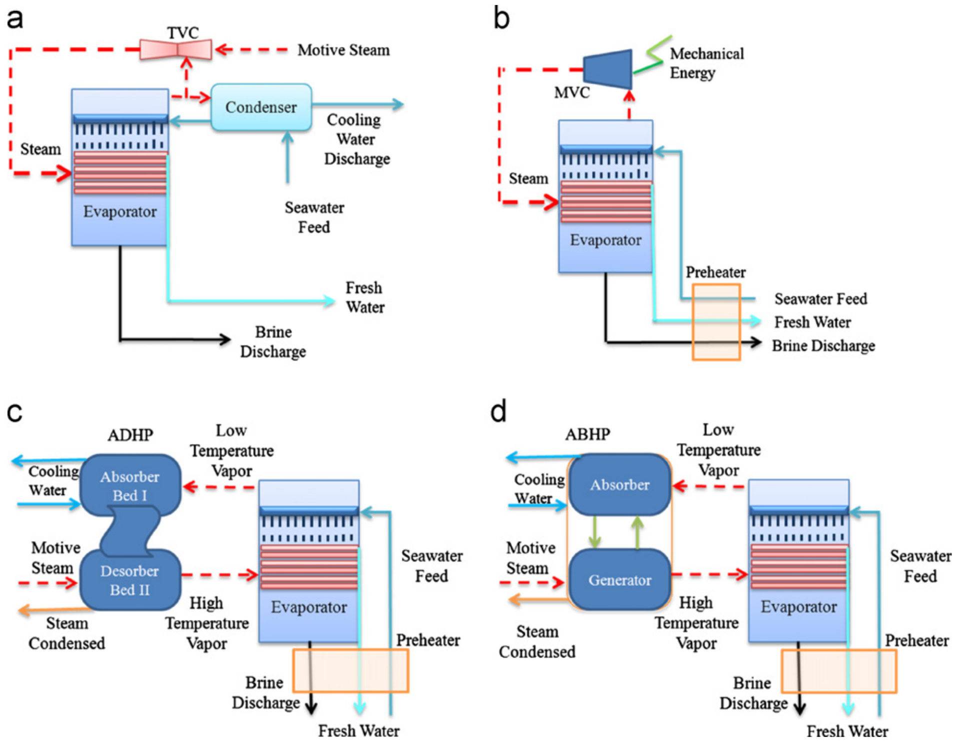

Fig. 7. Schematic of different heat pumps used in desalination. (a) Thermal vapor compression (TVC), (b) Single effect mechanical vapor compression (MVC), (c) Single effect adsorption heat pump and (d) Single-effect absorption heat pump.

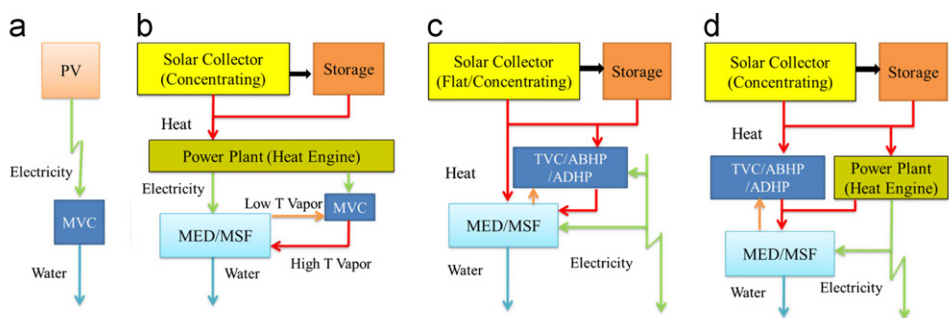

Fig. 8. Possible configurations for the solar assisted heat pumps and combinations.

energy recovery device such as a pressure exchanger [6]. Osmosis is a natural phenomenon in which water passes through a membrane from the lower salt concentration side to the higher salt concentration side. To reverse the flow of water, a pressure larger than the osmotic pressure must be applied. Seawater pressure must be higher than the natural osmotic pressure, typically 2500 kPa, but is kept below the membrane tolerance pressure, typically between 6000 kPa and 8000 kPa, forcing pure water molecules through the RO membrane pores to the fresh water side. Fresh water is collected while the concentrated brine is rejected. Among the reported solar assisted RO seawater desalination research, PV driven RO and solar thermal heat engine driven RO are the most widely studied.

2.4.1. *PV assisted RO system*

The PV powered RO system is very popular in demonstration plants [120–122] because both PV and RO are modular and easily scalable [123]. Considerable research has been carried out on whether to use (i) an energy recovery device [124]; (ii) a battery [125]; (iii) another power source, such as wind [126] or diesel [130], in a hybrid system; or (iv) another desalination method should be combined with RO to desalinate water [127]. A parametric study for economic analysis was conducted in [128] and optimization strategy was studied in [129]. Generally speaking, a PV–RO combination works like two independent units of PV and RO. Although there is still much room for improving the combination of both technologies, technical feasibilities normally are not the barriers as compared to the economic [130] and reliability considerations [131]. Table 9 lists a few selected seawater PV–RO and hybrid systems developed after the year 2000.

2.4.2. *Solar thermal assisted RO system*

Different from PV to RO plants which are almost commercially available in small scale and compact plants, solar-thermal RO desalination plants, as illustrated in Table 10, are still far from commercialization. Some researchers [140,141] have studied the application of solar thermal energy for desalination by coupling an organic Rankine cycle (ORC) with the seawater reverse osmosis (ORC–RO). The advantage of coupling an ORC with a desalination system is that the seawater provides a heat sink for the ORC condenser while at the same time it is preheated to increase

Table 7
Summary of Solar Thermal Desalination System Using Heat Pumps.

Authors	Solar Systems	Heat Engines	Other Desal. Systems	Heat Pumps	Desal. Cap. (m^3/d)	Notes
Zejli [99]	PTC		MED	ADHP		Modeling a conceptual desalination plant using 2 adsorption reactors and a three-effect MED
Palenzuela [109]	PTC	Steam Cycle	MED	TVC	48,498	Motive steam pressure is 2 bar, the PTC–MED–TVC system could compete with PTC+RO.
Sharaf [110]	PTC		MED	TVC	4,545	PTC–MED–TVC gives attractive results compared against
		Toluene ORC	MED	MVC	4,545	PTC–MED–MVC technique.
Helal [111]	PV			MVC	120	Solar/Diesel Hybrid
Nguyen [112]	Flat		Evaporator	ABHP		Hybrid gas/solar-driven absorption heat pumps showed higher water yield than conventional solar stills
Milow [106]	PTC		MED	DABHP[a]	72	Solar thermal desalination project (STP): Prove the technical feasibility of solar drive DABHP–MED system, cost $2/$m^3$
García-Rodríguez [107]	PTC		MED	DABHP	72–2,400	STP Project: DEAPH–MED suitable for solar application than MED only system due to the high energy cost delivered by solar field
Alarcón-Padilla [100]	PTC		MED	TVC DABHP	72	Summarized STP project which tested PTC driven MED, TVC–MED and DABHP–MED system. DABHP-MED is the most promising for solar driven desalination system which would further studied in AQUASOL project
Alarcón-Padilla [50,105,113,114]	CPC[b]		MED	DABHP	72	AQUASOL project: Experimental demonstrated the feasibility of the hybrid solar/gas desalination using DEAPH–MED. Reviewed past experience of DEAPH-MED and provided design suggestions.
Roca [115–117]	CPC		MED	DABHP	72	AQUASOL project: described and model control- feedback system
Gomri [118]	Flat		Separation-Condense	AHT[c]		Developed one computer program for modeling AHT-Distillation system and provided energy, exergy analysis.

[a] DABHP: Double effect absorption heat pump.
[b] CPC: compound parabolic concentrator.
[c] AHT: absorption heat transformer.

Table 8
Thermodynamic assessment of solar collector-MED desalination plants [100].

Desalination system	Main energy consum. (kJ/kg)(°C)	Solar desalination system	Solar energy consum[a] (kJ/kg)	Exergy performance of solar desal system[c](%)
DEAHP-MED	108 (at 180)	PTC–DEAHP–MED	142	4.3
MED	240 (at 70)	PTC–MED	315	2.0
MED	240 (at 70)	LTC–MED	545–1600	1.1–0.4
			333–369[b]	1.8–1.7

(PTC: parabolic trough collectors, LTC: low temperature solar collectors).
[a] Efficiency of solar collectors at solar irradiance of 800 W/m^2.
[b] If evacuated absorber tubes are used.
[c] Exergy of the distillated is 5.863 kJ/kg. Auxiliary energy consumption is not considered.

the RO membrane permeability, leading to reduced power consumption.

Kosmadakis et al. [141–146] did the pioneering research on integrating ORC with RO and were the only ones who carried out both theoretical and experimental studies. The solar collectors they used could provide up to 150 °C for the ORC using R245fa as the working fluid in a topping cycle while R134a as the working fluid for the bottom cycle. The recovery of their RO system was relatively low which was less than 20% while most seawater desalination plants operate with recovery at 35–60% [147]. Delgado-Torres et al. [148] pointed out that a single ORC with R245fa as the working fluid would have a higher efficiency than the cascade system studied by Kosmadakis et al. when operating between the same two temperatures. Tchanche et al. [149] pointed out that the integration of different devices is not significantly rewarded with an efficiency gain; therefore, it is preferable to keep the configuration of the ORC simple when designing an ORC–RO system.

The solar collector could be a flat plate or evacuated tube collectors (ETC) to provide heat source temperatures less than 150 °C or concentrating collectors for higher temperatures. The relative organic Rankine cycle should use different organic fluid in order to match the solar collector and the heat source temperature. Some high temperature (300–400 °C range) solar ORC driven desalination system working fluids could be [148,150–156]: toluene, octamethylcyclotetrasiloxane ($C_8H_{24}O_4Si_4$), decamethylcyclopentasiloxane ($C_{10}H_{30}O_5Si_5$), hexamethyldisiloxane ($C_6H_{18}OSi_2$) and tetradecamethylhexasiloxane ($C_{14}H_{42}O_5Si_6$). The later 4 compounds are usually referred to as D4, D5, MM and MD4M, respectively. Since RO needs only mechanical energy, which can be provided by a power cycle, the high temperature ORC cycles with higher efficiency could provide more mechanical energy per unit collector area. However, which kind of collector is the best needs to be analyzed case by case and will be affected by many factors such as the collector unit cost, location, etc. [157].

2.5. Solar assisted electro-dialysis

Electro-dialysis (ED), driven by electricity only, is a type of technology which arranges cationic and anionic ion-exchange membranes alternately in a direct current field (Fig. 10), where the salt ions migrate from the dilute solution side to the

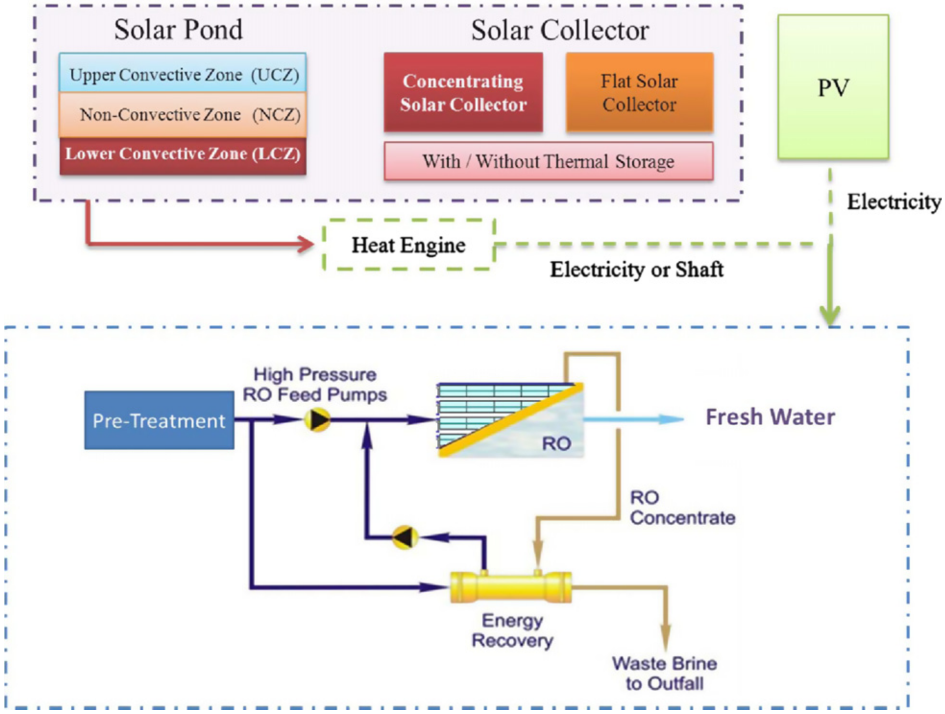

Fig. 9. Schematic of solar assisted RO process.

Table 9
Selected PV assisted RO seawater plant.

Systems (location)	Year	Additional power supply	Production (m^3/d)	Cost (\$/m^3)	Battery	Energy recovery system	PV capacity (kW)	Source
Abu Dhabi, UAE	2008	Diesel	20	7.2	No	Yes	11.25	[132]
		No		7.3	No	Yes	22.49	
Agriculture University of Athens, Greece	2008	No	0.35	7.8	Yes	Yes	0.85	[124]
	2004	Wind	12	5.2	Yes	Yes	30.22	[126]
		No	12	6.64	Yes	Yes	13.2	
CRES, Laviro, Greece	2004	Wind	3.12	31.5	Yes	No	4	[133]
ITC-DESSOL, Gran Canaria, Spain	2003	No	10	13.16	Yes	No	4.8	[134]
CREST, Loughborough University, UK	2003	No	3.9	2	No	Yes	2.4	[135,136]
CIEA-ITC, Canary Islands, Spain	2001	No	1.24	9.6	Yes	Yes	4.8	[137]
CRESTA, Curtin University of Technology, Australia	2007	Diesel	1	NA	Yes	No	1.2	[138]
GECOL at RasEjder, Libya	2005	Wind and grid	300	0.9	No	Yes	50	[139]

concentrated solution side through ion-exchange membranes under the influence of an applied electric potential difference. ED processes are different from the MSF, MED and RO systems in that dissolved salts are moved away from the feed seawater rather than the reverse. They are not economically competitive for seawater applications because of the large quantities of salt, the high cost of electrodes, the expensive ion exchange membranes and relatively short life time of membranes when working in a high-density electric field [160,161], therefore, most of the researchers used a PV driven ED process only for brackish water [162–165]. In a small scale 10 m^3/d PV driven ED plant experiment, the seawater needs to re-circulate a number of times before the desired water quality is obtained [166,167]. So far, only a few studies have been carried out on solar assisted ED seawater desalination [168,169].

2.6. Solar assisted passive vacuum desalination (PVD)

The passive vacuum desalination (PVD) concept is to use a thermal system without using a steam ejector or vacuum pump in a small scale thermal system application, as originally adopted by Goswami [170,171] for desalination applications. The basic concept as seen in Fig. 11 is that a thermal system is first filled with seawater to a height of more than 10 m above the ground, then the water drains to create vacuum in the system. The vacuum is generated in the headspace left in a sealed tank taller than 10 m when the standing column of water held by atmospheric pressure drops by gravity. Detailed description and analysis may be found in Refs. [172–174] in which both theoretical modeling and experimental results are provided. Several researchers have used this idea as the basis and further developed different passive vacuum systems such as systems combined with sensible heat thermal energy storage (TES) [175,176], combined with wind power [177], and combined with PV system [178] etc., as listed in Table 11. Though the passive vacuum method could generate vacuum by using natural gravity without using vacuum pumps, the non-condensable gases within the seawater can accumulate over time and affect the vacuum conditions in the evaporator, which lowers the overall heat transfer efficiency and reduce the fresh water production rate [171,179,180]. In summary, PVD is a

Table 10
Summary of Solar ORC driven seawater RO research.

Author	Experiement or model	DNI (W/m^2)/ location[a]	Cycle highest temperature	Cycle fluids	Cycle configuration	Pressure (bar)	RO pressure (bar)	Cycle efficiency	Collector area per kg fresh water (m^2/L/s)	Feed salinity (ppm)	Recovery rate [o]
Manolakos [145]	Model	Athens, Greece	75.8	134a	Single ORC	22	47.8	0.73–3.08	864[b]/648[m]	42710	0.18–0.2
Manolakos [143,158]	Experimental	1000	75.8	134a	Single ORC	22	47.8	7	1056[C]/792[m]	42710	0.15
Kosmadakis [142,144,159]	Model	1000	137	245fa	Cascade upper cycle	26.6	56.2	11.8	432[d]/324[m]	42710	0.2
			75.8	134a	Cascade bottom cycle	22					
Delgado-Torres [151]	Model	850	355.7[i]	Toluene	Cascade upper cycle	<41.26[j]	55.3	21.29[i]	48.2[e,f,i]	35731	0.488
			129.8–130.3[i]	Isopetene	Cascade bottom cycle	<33.78[j]	55.3	10.59–13.06[i]			
			336.3[i]	MM[n]	Cascade upper cycle	<19.39[j]	55.3	15.33[i]	65.2[e,f,i]		
			145[i]	Isopetene	Cascade bottom cycle	<33.78[j]	55.3	10.93–13.44[i]			
Delgado-Torres [150]	Model	850	320–380[i]	Toluene	ORC with Recuperator	<41.26[j]	NA	29.48–31.78[i]	NA	NA	NA
			260–380[i]	MM	ORC with Recuperator	<19.39[j]	NA	23.87–25.93[i]	NA	NA	NA
Delgado-Torres [148]	Model	1000	145[l]	R245fa	ORC with recuperator	20.866	52.4	15.46	73.7[e,f]	35700	0.45
Bruno [157]	Model	800	87.3	R218	ORC with recuperator	<26.8[j]	64.8	7.81	1209.6[b,g,h]	36000	0.5
			120.9	R245	ORC with recuperator	<31.37[j]	64.8	13.24	603.1[b,g,h]	36000	0.5
			289.7	R601a	ORC with recuperator	<33.7[j]	64.8	27.61	336.0[b,g,h]	36000	0.5
			378.4	*N*-propyl benzene	ORC with recuperator	<32[j]	64.8	32.19	231.8[b,g,h]	36000	0.5
A.S. Nafey[k] [140]	Model	850	100	water	Rankine	0.576	67	10.17	449.4[d]	45000	0.3
		850	150	water	Rankine	2.755	67	13.34	402.5[d]	45000	0.3
		850	320	Toluene	Single ORC	32.78	67	26	166.3[d]	45000	0.3

[a] DNI is direct norm radiation which is used for modeling design, location is experimental or case study location and solar radiation data TM2 is used.
[b] Gross collector area calculated by TMY2 data.
[c] Gross collector area from experimental data.
[d] Gross collector area caculated by design DNI data.
[e] Aperture area of collector calcuated by design DNI data.
[f] Use 24 h a day to convert from daily flow data.
[g] Use 7 h a day to conver daily flow data.
[h] Case study results for location Barcelona.
[i] Data for LS3 collector using heat transfer fluids.
[j] Critical pressure of the fluids.
[k] Data selected from superheat condition.
[l] R245fa using heat transfer fluids with recuperator effective factor 0.8.
[m] Convert to Aperture area.
[n] MM is Hexamethyldisiloxane.
[o] Recovery rate refers to the percentage of the feed seawater that is recovered as fresh water.

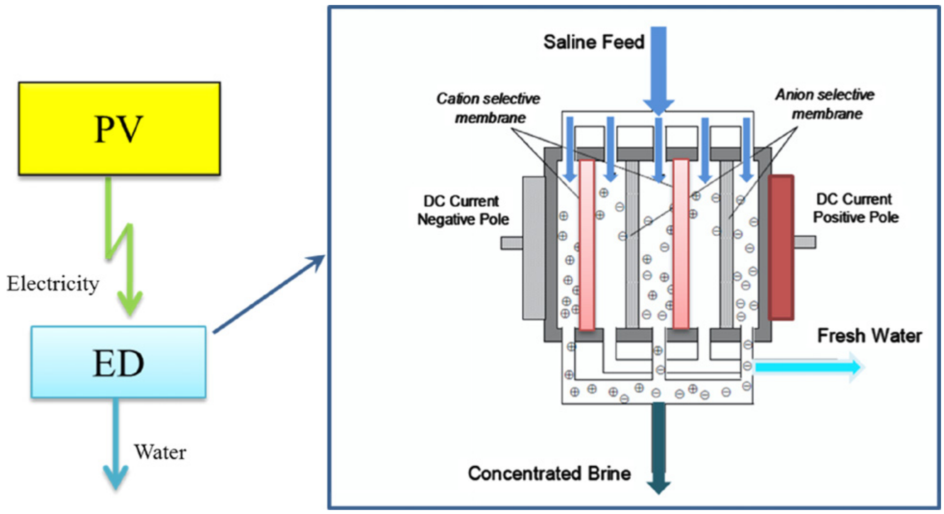

Fig. 10. Schematic diagram of PV assisted electro-dialysis desalination process.

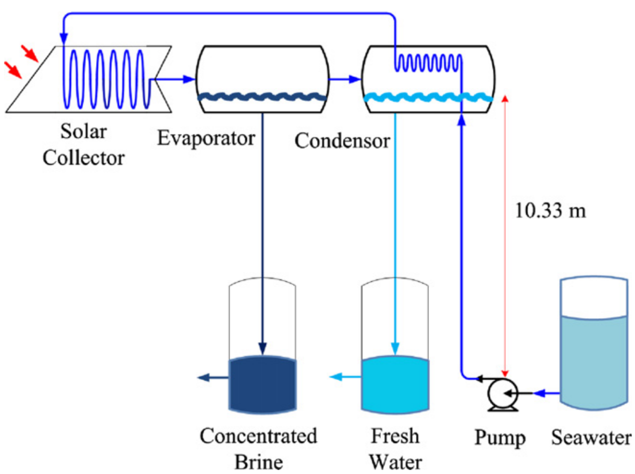

Fig. 11. Single-stage passive vacuum flash desalination system.

simplified MSF/MED thermal system and could operate with less pretreatment compared to the RO. It is suitable for places like ships where the deck height is naturally more than 10 m higher than the seawater level and where robust desalination systems are needed.

Table 11
Research on passive vacuum desalination system.

Authors	Year	Comments
Goswami [170,171,179]	2003 2004	Proposed and built evaporation based PVD concept using solar water heater; experimental analysis confirmed theoretical modeling which showed that the effect of withdrawal rate and the depth of water in the evaporator were small while the effect of heat source temperature is significant.
Nirmalakhandan [175,176]	2008	PVD combined with sensible thermal storage system and solar absorption air-conditioning system. Simulation showed an energy consumption less than 210 kJ/kg freshwater produced
Goswami [173,174,180]	2009 2010	Proposed and built flash system based PVD system. Experimental results showed process is feasible if operated at high temperatures and moderate flow rates. However non-condensable gas accumulation reduced water production rate.
Ayhan and Madani [177]	2010	PVD desalination system combined renewable energy such as wind power and solar power giving a production cost of $1.00 per ton for a lifetime period of 20 years
Nirmalakhandan [178]	2010	PVD combined with solar still and PV panel system. Experiments showed that the system could produce two times of the distillate than simple solar still.

2.7. Solar still

In a solar still, also called direct still system (Fig. 12), the heat collection and distillation processes occur within the same system where solar energy is used directly for distillation by means of the greenhouse effect. Water vapor rises to the transparent cover by natural convection and condenses there. A solar still output might be affected by many factors including brine depth, vapor leakage, thermal insulation, cover slope, shape material, climate [181,182]. The latent heat is normally wasted on the cover, therefore the system efficiency is relatively low with a daily production of about 3–4 l/m^2 [44].

Solar stills have been extensively studied [202], as listed in Table 12. A theoretical relationship of heat and mass transfer within the still was developed by Dunkle [203]. Later, researchers developed different kinds of solar still systems, such as: solar stills coupled with solar collectors, as can be seen in Fig. 12b [183–186]; solar stills with condensers (Fig. 12c) [187,188]; solar stills under low pressure [189,190]; solar stills with heat recycling [191,192]; multi-stage/multi-effect solar stills (Fig. 12d) [193–195]; solar stills with heat storage [196–199]; and hybrid solar still/PV systems [200,201].

2.8. Solar assisted humidification–dehumidification (HDH)

The HDH process, which uses low grade heat that could be supplied by solar collectors, is based on the fact that the saturation humidity roughly doubles for every 10 °C increase in temperature. For example, air at 90 °C can hold five times more water than air at 70 °C. When air comes in contact with salt water, it extracts some amount of vapor at the expense of sensible heat of salt water, causing cooling. On the other hand, the distilled water is recovered by maintaining humid air in contact with the cooling surface, releasing the latent heat of condensation from the vapor. HDH can be divided into two big groups: closed air, open water (CAOW) cycle and closed-water open-air (CWOA) cycle [204,205]. More detailed system configurations, combinations and modeling

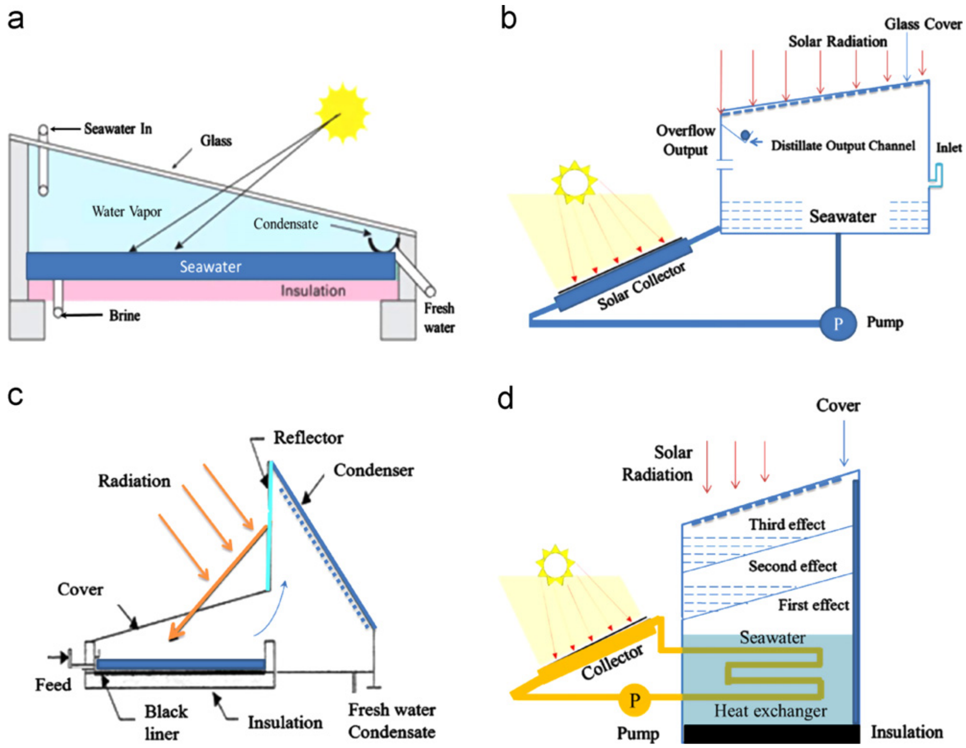

Fig. 12. Schematic of solar still (a) Single stage solar still (b) Solar still with collector (c) Solar still with condenser (d) Multi-stage solar still.

Table 12
Selected solar still desalination systems.

Main feature	Author	Additional comments
W/collector	Kumar [183]	Water flow over the cover to increase the temperature difference
	Lawrence [184]	System was operated under thermosiphon mode
	Tiwari [185]	thermal analysis showed that efficiency drop with increase of collector area
	Yadav [186]	Numerical analysis agrees well with experimental results
	Badran [187]	Coupled with flat collector and studied parameters (i.e., water depth, direction of still, radiation)
W/condenser	El-Bahi[187]	Output increased 70%
	Fath [188]	Output increased 50%
W/vacuum units	Tay[189]	uses waste heat from steam turbine
	Low [190]	Use turbine exhaust steam
W/heat recovery	Mink [191]	Both latent heat and sensible heat to pretreat feed
	Schwarzer[192]	recover latent heat from the condensation process
Multi-stage/effect	Fernandez [193]	Each tray has a W-shape bottom that acts as a condenser for the pan below
	Kumar [194]	Numerical model was developed and validated for a single effect still
	Tanaka[195]	vertical multiple-effect diffusion-type still with solar collector,
Heat storage	El-Sebaii [196]	phase change material (PCM) was used for heat storage
	Onyegegbu [197]	Still with thermal energy storage
	Velmurugan[198,199]	Solar stills integrated with a mini solar pond
Hybrid system	Kumar[200]	Waste heat from PV system for water heating
	Hidouri[201]	solar still connected to a heat pump

could be found in Ref. [206]. Among all kinds of configurations, the multi-effect CAOW water-heated system is regarded as the most energy efficient [207]. The schematic of one solar assisted multi-effect CAOW can be seen in Fig. 13. The basic cycle has a solar collector as the heat source, an air humidifier and a dehumidifier. Seawater passes through the collector where the temperature rises and then through the humidifier where water vapor and heat are given up to the counter-current air stream which cools down the brine. Finally the air passes over the dehumidifier where fresh or sea water is used for cooling.

The HDH process is still under research and development and there is still a lot of room to improve the process [208,209]. Researchers have produced experimental results to verify the models [210–213], have tried different methods including studying the ambient temperature effect [214], developing corrosion free HDH collectors [215], combining a cooling tower to improve water production [216], using pinch analysis to improve the system performance [217,218], and adjusting the seawater/air flow ratio to maximize water production [219,220], etc.

It should be noted here that the predecessor of the single stage HDH cycle is a simple solar still whose energy cost is very high [221]. Therefore, theoretically, this system should be targeting small-scale applications [220] (from 5 m^3/d to 100 m^3/d water production) for which the cost of water production is much higher than for large-scale systems. Several cost estimations and optimizations are given in Refs. [222–224] with mixed results on whether or not HDH is more economical than small scale RO as reported in Refs. [82,225].

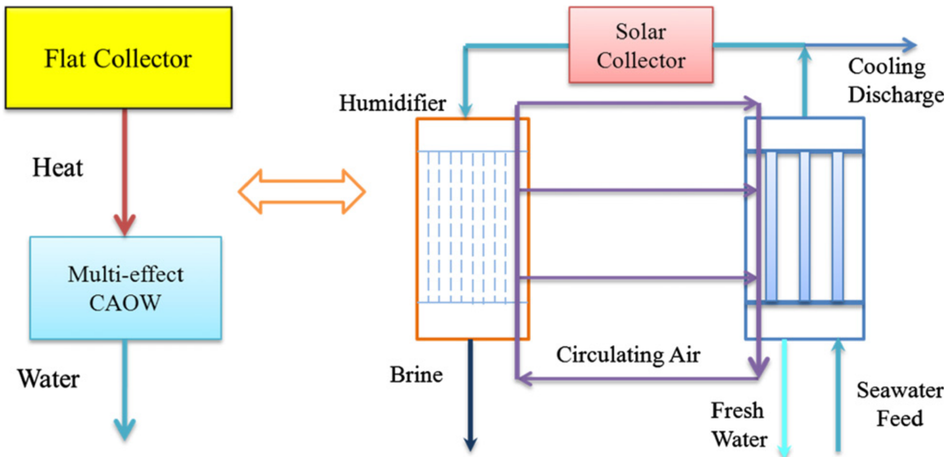

Fig. 13. Schematic of solar assisted multi-effect CAOW system.

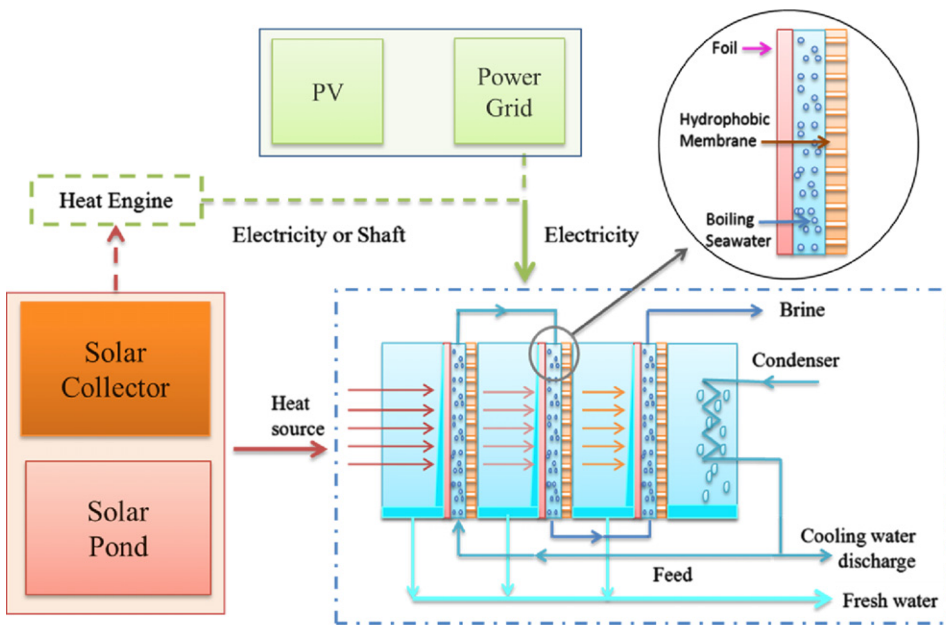

Fig. 14. Schematic of solar assisted membrane distillation.

2.9. *Solar assisted membrane distillation (MD)*

Membrane distillation (MD) desalination requires both thermal energy and mechanical energy; therefore its combination with solar energy is similar to the solar assisted MSF/MED process, as shown in Fig. 14, which could use low grade heat from solar collectors or a solar pond, electricity from a PV system or the power grid. MD is a separation process in which a hydrophobic, micro-porous membrane is used with seawater on one side of the membrane and condensing vapor on the other side. The hydrophobic membrane prevents seawater from passing through the membrane pores and only allows the generated vapor transfer to the other side. MD is a thermally driven process. The driving force is the partial pressure difference across the membrane. There are four kinds of configurations: direct contact membrane distillation (DCMD); air gap membrane distillation (AGMD); sweeping gas membrane distillation (SGMD); and vacuum membrane distillation (VMD). Detailed descriptions could be found in Ref. [226].

As for the MD energy consumption and cost, there are some disagreements among the researchers. Some believe that [227] MD is unfavorable when compared with MED and MSF from an energy utilization point of view because of the additional resistance to mass transport and reduced thermal efficiency (due to heat conductivity losses) offered by the membrane, while others claim that the MD consumption is comparable to that of MSF plants but the pumping power is less [228]. Nevertheless, by using novel materials and by optimizing the MD configuration, one could simultaneously reduce the temperature polarization and permeability obstructions of salt solutions in the DCMD [229], which might potentially reduce the cost. In addition, MD uses membranes that are robust and cheap, which means that MD could save on the chemical usage and the seawater pretreatment costs compared with RO [230]. Some selected solar assisted MD seawater desalination systems can be seen in Table 13, in which most solar assisted MD systems operates at temperatures less than 80 °C. MD driven by a solar pond has been shown to be feasibile; however, modeling results have shown that combining solar collectors with the MD system could achieve a higher membrane permeate flux [231]. Though there are many cost estimations for MD desalination, there are only a few reports on solar MD seawater desalination costs. Banat et al. [232] estimated the water cost in the project "SMADES" as \$15/m^3 for a 100 l/d

Table 13
Selected solar assisted MD seawater desalination systems.

Ref.	Mod/ exp.	Project	MD type	Solar system	Cap. (m^3/d)	Notes
[31], [285]	Mod/ exp	El Paso	AGMD	Solar Pond	0.35	3000 m^2 solar pond, production 0.0016 m^3/d/m^2 of SGSP.
[232,233], [256,257], [286,287],	Exp.	MEMDIS, SMADES	DCMD	FPC–PV	0.1–0.5	Compact single loop MD systems using 5.73–7 m^2 FPC, 7–12 m^2 membrane area, GOR 3–6; Experiments carried out at Pozo Izquierdo (Grand Canary), Alexandria (Egypt), Irbid (Jordan), Morocco and Freiburg (Germany), Tenerife (Spain)
					0.9	Two loop systems using 72 m^2 FPC, 1.44 kW p PV, 3 m^3 water tank, batter storage,4 membrane modules, freed salinity 55000ppm, RR 3–4.5%, experiments at Aquba, Jordan
					1.6	Two loop systems using 90 m^2 FPC, 4 m^3 water tank, 1.92 kW p PV, no battery,5 membrane module, PV for pumps, two loop systems, double glass collector with anti-reflective coating, feed water 35,000 ppm, RR 3.6%
[231]	Model[c]	MEDINA	VMD	Solar pond	[d]	High fluxes of 140 L/h/m^2 could be reached (for a vacuum pressure of 500 Pa and a membrane with a Knudsen permeability of 1.85×10^{-5} s/$mol^{0.5}$/m/$kg^{0.5}$).
[288]	Exp.		NA	Solar still	NA	The effect of salt concentration on the membrane flux and the solar still was marginal; the contribution of the solar still in the distillate production was no more than 20% in the outdoor tests and less than 10% in the indoor tests.
[289]	Model/ exp.	SMDDS	AGMD	FPC	0.64–0.71[a]	Develop a model for SMDDS, FPC absorber area 72 m^2, membrane area 10 m^2, spiral wound AGMD structure; the use of a storage tank, an interior coil heat exchanger and a control system using conventional Proportional/Integral controllers could improve the system performance.
[290]	Model[c]	MEDESOL	AGMD[b]	CPC	0.5–50	Laboratory tests under defined testing conditions of all components will be performed in Spain and Mexico

[a] Simulated results.
[b] Authors mentioned that the experimental MD system will be AGMD modules while DCMD and VMD will also be theoretically analyzed.
[c] Experiments in progress.
[d] Model maximum fresh water production 617 L/h.

system using a 10 m^2 membrane and 5.73 m^2 flat panel collectors (FPC), and \$18/m^3 fora 500 l/d system FPC–PV driven MD using 40 m^2 membranes and 72 m^2 FPC [233], and showed that by increasing the reliability and plant lifetime the cost could be further reduced.

Overall, solar assisted MD is still under development stage. Reports on novel processes [234], experimentally confirmed modeling [235] and pilot demo plant evaluations [236] continue to appear in the literature. MD has the disadvantage compared to MED and MSF of additional resistance to mass transport by the membrane [227]. However because of the lower cost of MD materials, this disadvantage can be compensated by using more area for heat and mass transfer. In addition, it could be used for high recovery or highly concentrated salt water treatment, that RO could not handle, which normally require high energy consumption.

3. Discussion

There are many kinds of desalination processes as well as solar technologies. Selecting a suitable desalination process for sea water requires several design criteria including seawater quality, capital cost, operation and maintenance cost, energy efficiency, water quality requirements, environmental impact and other site specific factors [237,238]. Selecting a suitable solar system requires a number of considerations, such as, location, energy storage method, operating temperature range, type of solar collector, working fluids, plant configuration, etc. [239]. When coupled together, though some systems requires some minor changes for better integration, most of the reported solar desalination systems are not developed as a single system but are integrations of components developed independently [240].

3.1. System integration based on energy type

Fig. 15 shows potential processes of solar technologies combined with seawater desalination technologies. Generally speaking, solar assisted desalination system means that either solar energy is converted to electricity in order to power the RO/MVC process, or that solar radiation is collected by thermal collectors and this energy is used for the thermal desalination process. Solar methods which mainly produce electricity, such as photovoltaic (PV), solar chimney [241], etc. are suitable to be combined with the membrane desalination process or a thermal process like MVC which only uses mechanical energy. Other solar technologies such as solar pond, solar collectors including FPC, ETC, CPC, PTC, solar dish, fresnel reflector, solar tower etc., which could be used to generate electricity and heat at the same time, could be combined with any kind of desalination technology based on the design. Since both solar and desalinations systems are developed independently and then coupled together, it is necessary to analyze them separately.

3.2. Desalination system considerations

In order to select the best solar-desalination integrated system, understanding of desalination minimum energy requirements, energy recovery and major exergy destruction processes is important. One review, specifically focusing on energy issues of desalination, can be found in Ref. [242].

3.2.1. Minimum energy requirement for desalination

Minimum energy is required when the salt and water could be separated in a completely reversible process irrespective of the actual desalination processes [242,243]. With the development of modern tools and information available in the literature [244–246], it is now much easier to calculate the minimum energy than before. In a reversible process, the minimal work required for the separation of water from seawater is the difference in the Gibbs energy [84]

$$w_{min} = \frac{m_{br}g_{br} + m_w g_w - m_{sw}g_{sw}}{m_w} \tag{1}$$

$$g = h - TS \tag{2}$$

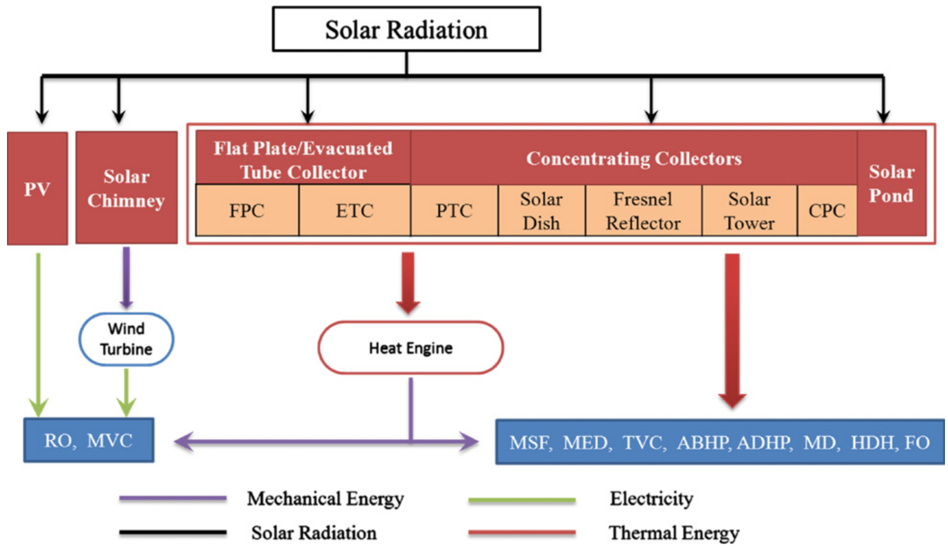

Fig. 15. Potential process of solar desalination.

where subscripts *br*, *w* and *sw* represent rejected brine, produced fresh water and feed seawater (35,000 ppm), and *g* is the specific Gibbs energy. The results can be seen in Fig. 16((a) and (b)), which showed that higher salt concentration and higher recovery rate require higher energy consumption. Based on the above equations, at 25 °C, standard seawater (35,000 ppm) with 50% recovery, the reversible process requires 3.93 kJ/kg. The current well designed seawater RO systems or controlled pilot scale plants energy consumption can be as low as ~7.92 kJ/kg [247], which is 2 times the minimum required theoretical value. Considering pretreatment, post-treatment or other factors such as membrane fouling, pipe friction losses, pump efficiency, etc., there is only about 20% improvement possible [247].

3.2.2. Recovery rate for seawater desalination process

Low recovery consumes less energy in the separation process but consumes more in pumping; therefore there is an optimized range for the seawater recovery. The work required for the RO process with an energy recovery device (EDR) may be estimated by

$$W_{SWRO} = \frac{V_{fresh}}{\eta_{pump}} \times \left(\frac{P_{sea}}{1-\alpha} + \Delta P\right) \times \left[1 + \left(\frac{1}{\alpha} - 1\right) \times (1-\eta_{ERD})\right] \quad (3)$$

where α is the seawater desalination system recovery ratio, ΔP is the overpressure above the osmotic pressure that drives the water flow through the membrane; P_{sea} is the osmotic pressure given by van't Hoff equation: $P_{sea} = cRT$ where c is the ionic molar concentration, R is the gas constant, and T is the absolute temperature; and $\frac{P_{sea}}{1-\alpha}$ is the pressure used to overcome the concentrated brine osmotic pressure. The units of W, P, and V are kJ, kPa and m^3 (or m^3/s if using flow rate), respectively; η_{pump} is the high pressure pump efficiency, V_{fresh} is the fresh water volume and $\frac{V_{fresh}}{\alpha}$ is the total seawater pumped by the pump, and η_{ERD} is the efficiency of ERD. The recovery rate ranges from 30% to 60% for RO, as can be seen in Fig. 17. For thermal processes, the high recovery rate could reduce the energy consumed by the pumps but might cause potential scale problems, therefore, a selection needs to be made for each individual case.

3.2.3. Estimation of energy consumption

In this section it is not intended to show accurate energy consumption calculations but to provide a simplified method for the estimation of the energy use in a desalination process. As Fig. 18 shows, for any desalination process the final products are brine, fresh water and vapor (same temperature with fresh water which needs to be cooled by cooling seawater). Thermal energy and/or mechanical energy will be consumed. Assuming there is no heat loss to the

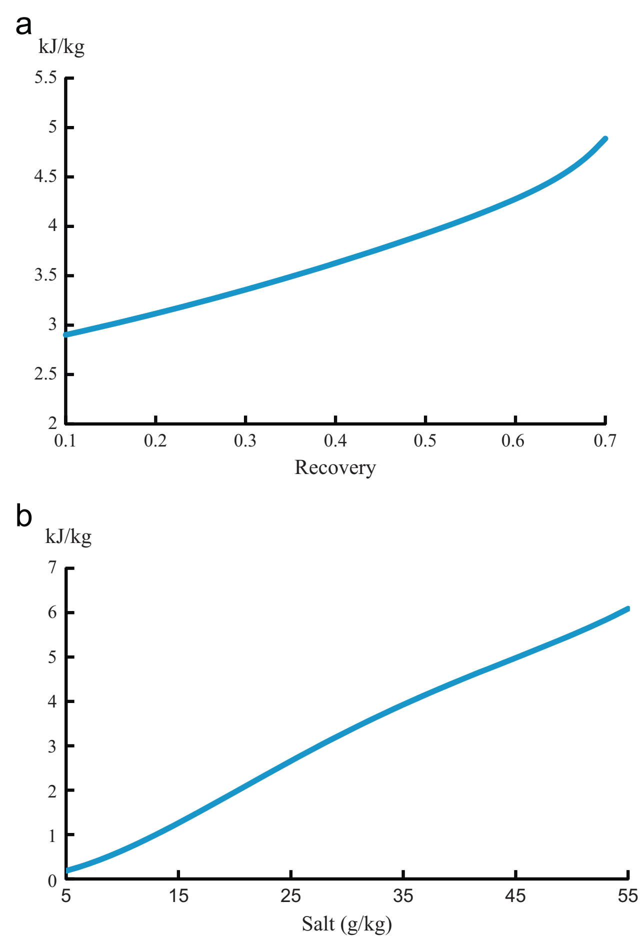

Fig. 16. (a) Minimum energy required to desalinate seawater versus recovery rate (35 g salt/kg seawater at 25 °C) and (b) Minimum energy required to desalinate seawater versus seawater concentration at 25 °C.

environment, when a desalination process uses heat only, W is zero. When only electricity is used, Q_{input} is zero. Based on mass and energy balance, the recovery rate could be expressed as

$$\alpha = \frac{m_f}{m_s} = \frac{\frac{(Q_{input}+W)-Q_{loss}}{m_s} + (h_s - h_b)}{(h_{fl}-h_b) + \frac{m_{fv}}{m_f}\lambda} \tag{4}$$

where h_{fl}, h_b, h_s are the specific enthalpy of fresh water vapor, concentrated brine and feed seawater, respectively, α is the recovery rate, λ is the latent heat at the final product temperature; m_{fv} is the fresh water vapor mass, m_f is the sum of the mass of the final fresh water production which is the sum of vapor stream F_v and the final fresh water stream F_L. If we define the specific energy consumption for a general desalination process as $q_s = \frac{Q_{input}+W}{m_f}$; assume the feed seawater at 25 °C and the final products having the same temperature including vapor, liquid fresh water and brine without considering the temperature elevation caused by salt, Eq. (4) could be

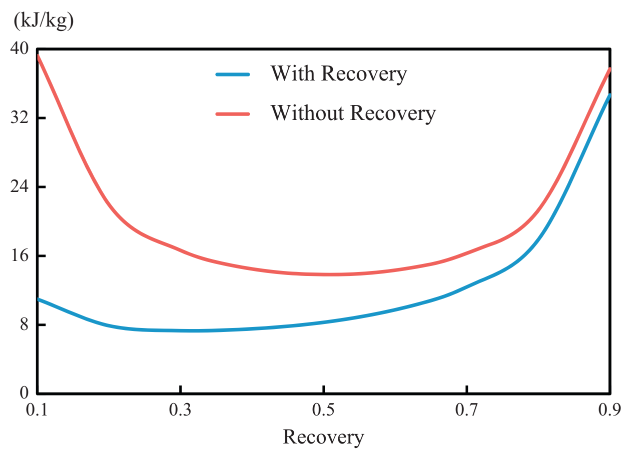

Fig. 17. Specific energy consumption change with/without ERD (pump efficiency 80%, ERD efficiency 80%).

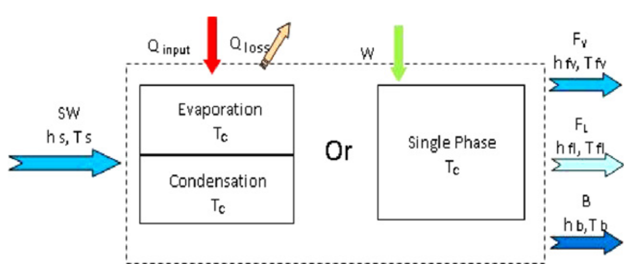

Fig. 18. General overview of a desalination process.

simplified as

$$q_s = \left[(h_{fl}-h_b) - \frac{1}{\alpha}(h_s - h_b)\right] + \frac{m_{fv}}{m_f}\lambda \tag{5}$$

where $\frac{m_{fv}}{m_f}$ is vapor ratio which showed the vapor amount of the total final fresh water generated; R is the recovery of the desalination process. Once the recovery, α, is fixed, the specific energy is directly related to the amount of vapor condensed by the cooling water which is discharged to the environment. Fig. 19 shows the estimated specific energy consumption with vapor fraction of the total fresh water generated. The lower the amount of vapor condensed by the discharged cooling water, the lower the energy it requires because less latent heat is wasted. This estimation shows that the RO process stands out among others because it uses almost ambient conditions to generate fresh water, no vapor needs to be condensed and no cooling water is needed. Other processes, i.e., MED, MSF, MVC, MD, HDH, etc. could reduce the energy consumption by recovering the latent heat of the generated vapor either by preheating water or by reusing the latent heat so as to reduce the energy wasted in the cooling water. For single effect thermal processes, the vapor ratio is 1. Recently forward osmosis which makes use of the osmosis by extracting water from seawater using a concentrated extraction solution (also known as draw solution), has gained attention [248]. One of the draw solutions proposed is a mixture of NH_3, CO_2 and water which extracts fresh water from seawater by forward osmosis. Fresh water is then gained from this solution by heating, decomposition, and the stripping and recycling of the ammonia and carbon dioxide gases [249]. They claimed that the energy savings of FO are projected to range from 72% to 85% compared to current technologies on an equivalent work basis [249]. However, the model and the equations used in the commercial software packages are not clearly stated. Regardless, this process still depends on phase change therefore some researchers questioned some claimed advantages of this method [242].

3.2.4. Energy reduction in desalination processes

Although different desalination processes share the same minimum power requirements, independent of system configuration and technologies, it is not practical to operate systems reversibly to achieve the minimum energy consumption. Different driving forces for different desalination processes could cause different exergy destructions. A higher driving force leads to a higher water production rate but with higher exergy destruction, which normally leads to smaller systems but with higher energy consumption. The driving force of different desalination systems are: the excess pressure ΔP for RO, the excess voltage ΔE for ED, the additional temperature difference ΔT in excess of the boiling point elevation to allow for heat transfer for MVC and MED and the additional temperature ΔT in excess of the boiling point

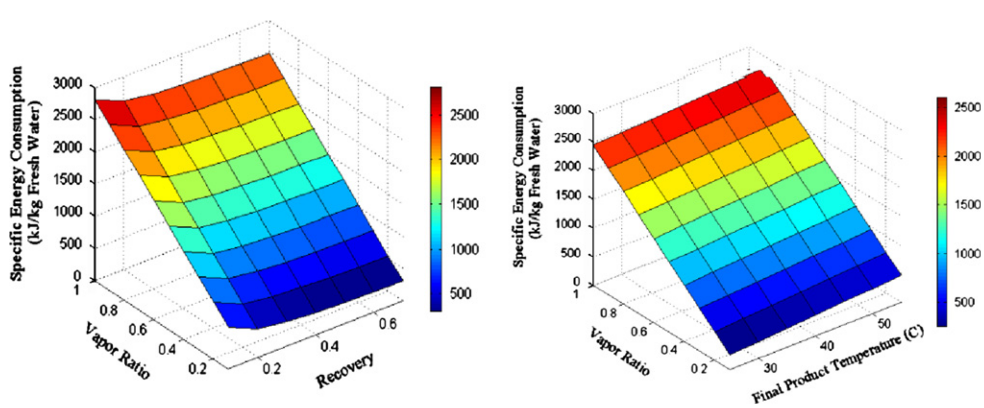

Fig. 19. Specific energy consumption with vapor ratio and recovery when final product is at 35 °C (left); and final product temperature when recovery is 0.5 (right).

Table 14
A Comparison of different desalination processes. [258–260].

	MSF	MED	TVC	MVC	RO	ED
Operation temperature (°C)	35–120	35–100	> 120	30–60	20–40	20–40
Pretreatment requirement	low	low	low	low	high	high
Scale problem	High	Medium	Medium	Medium	Low	Medium
Freshwater quality (ppm TDS)	< 10	< 10	< 10	< 10	350–500	350–500
Heat consumption (kJ/kg of product)	90–567	108–432	–	–	–	–
Electricity consumption (kJ/kg of product)	7.2–18	5.4–10	–	28–40	10–47	43
Prime energy consumption* (kJ/kg of product)	110–653	110–369	–	80–110	65–120	144
Energy recovery	Sensible to latent	Latent to latent	Recovery low temperature vapor	Recovery low temperature vapor	Pressure recovery	–
Sensible to feed in seawater temperature	Yes	No	No	No	No	No
Others	Proven technology for large scale plant	Proven technology	Steam temperature > 120 °C, sacrifice power plant performance	Limited to smaller size plants, need skillful operator	Membrane replace every 5–7 years, cannot treat high salinity water	Almost all brackish water application

Table 15
Solar system costs as percentages of the total solar desalination system costs.

Ref.	System configuration	Desal. cost (%)	Solar system cost (%)	Others cost (%)	Notes
[143,145,158]	Collector+ORC+RO	32	40	27	Working fluids 134a, cycle high temperature 75.8 °C
[142,144,159]		23.36	40.83	35.81	245fa top cycle fluids, 134a bottom cycle fluids, cycle high temperature 137
[140]		8.8[a]	71.7[a]	19.5	R218 as working fluids, cycle high temperature 87.34 °C
		7.2[a]	76.7[a]	16.1	R245 as working fluids, cycle high temperature 120.94 °C
		12.5[a]	59.6[a]	27.9	R601a as working fluids, cycle high temperature 289.73 °C
		18.5[a]	48.5[a]	32.9	*N*-propyl benzene as working fluids, cycle high temperature 378.44°C
[23]	Solar Pond+MSF	72.8	27.2	0	
		74.5	25.5	0	
[24]		26.7[b]	18[b]	55.3	
		25.1[b]	17.4[b]	57.5	
[22]		34.3[c]	59[c]	6.7	
		43.1[c]	50.2[c]	6.7	
[39]	Collector+MSF	27[d]	66.67	6.33	
		30[d]	60	10	
[81]	Collector+MED	20.09	73.78	6.1	
[126]	PV+RO	19	27	54	
[261]	PV+RO	69	31[e]	NA	
[142]	PV+RO	61	39[f]	NA	
[82]	Collector+HDH	NA	28	NA	

[a] case study results for location Barcelona.
[b] Interests, which are 7% for 15years, are not included.
[c] O&M cost is not considered.
[d] Only evaporator cost is considered, plant life=20 years. Annual operating 300 days and interest rate is 5%.
[e] Without batteries
[f] With batteries.

elevation to allow for flashing for MSF [250]. The general form is given by [251]

$$\frac{dE_d}{dt} = -T_0 \times \frac{d\Delta S}{dt} = -T_0 * (\Im * \Delta X) \qquad (6)$$

where E_d is the exergy destruction, t is time, ΔS is the entropy change, $\Im$ is a flow rate, T_0 is the environmental temperature and ΔX is the generalized driving force conjugated to the flow $\Im$. Assuming the plant and other conditions are equal, in order to reduce the exergy loss, the driving force needs to be reduced requiring a larger “reaction” area with larger capital cost. Theoretically, a thermal process like MED or HDH could contain more than 100 stages/effects [252,253]. In reality, the size of the desalination system and the energy consumption must be balanced. Modern large scale thermal desalination plants could have the temperature difference between adjacent stages as small as 2 °C. Considering the seawater boiling point elevation (about 0.5–1 °C) and saturation temperature drop (caused by pressure drop in the demister and tube), the net driving force of adjacent effects has approached 1 °C already; as for the membrane process, the current seawater RO plants could use a pressure only 10 to 20% higher than the osmotic pressure of the concentrate [247]. Therefore, reduction of the driving force in order to reduce the exergy destruction and the energy consumption is a necessary but challenging topic. Desalination is intensive in both energy consumption and capital investment. The water cost is a trade-off with energy and equipment cost. By using large areas of membranes in RO/MD or more stages/effects in MSF/MED, energy demands could be reduced buta higher cost. If a low cost RO membrane and heat exchanger were available, energy

consumption could be potentially reduced by using more material while maintaining the capital cost at a reasonable range. For example, even though the MD process uses a similar configuration as the MED or the MSF, it has the disadvantage of additional resistance to mass transport and reduced thermal efficiency (due to heat conductivity losses). However, it could exploit the advantages of a larger surface area to compensate for these disadvantages and still maintain a competitive capital investment [227]. Composite porous organic/inorganic membranes could have the potential to increase the heat conductivity and be used in a MD system. For the RO process, novel membranes presenting better flux, better rejection to salts and boron could also reduce the energy needed. The capital investment could also be reduced by using fewer membranes with higher flux and rejection abilities.

In summary, the minimum energy required for all the desalination processes is the same irrespective of the actual desalination processes. The RO process is naturally more energy efficient than a thermal process. However, the RO process could not be used to handle highly concentrated salt water such as fracture water generated from natural gas production due to the exponential increase of osmotic pressure with salt concentration and the physical strength limitations of RO membranes. Therefore in some cases, such as availability of abundant low cost thermal energy, highly salty water or places requiring zero liquid discharge, thermal processes could be more appropriate. The desalination cost could be further reduced by not only applying low cost energy sources but also low cost materials, which requires breakthroughs in materials development. Table 14 summarizes a comparison of some of the major desalination processes.

3.3. Solar system considerations

The solar system costs could range from 17.4% to 76.7% of the total system costs based on different system combinations, as can be seen in Table 15. With the exception of the solar pond driven desalination system which do not need solar collectors, all other configurations have more than 25% additional cost spent for the solar collectors. A solar pond requires a large surface area and the pond evaporation rate sometimes exceeds the water production rate, which makes it unsuitable for places with limited water resources [254]. As for the solar assisted ORC driven RO process, the exergy analysis shows that for the ORC–RO system the exergy destruction in the power plant is almost ten times greater than that in the RO subsystem [255], which indicates that the overall efficiency depends more on the solar plant and less on the desalination system. Overall, the solar system is a very large part of the overall system cost and needs to be carefully selected. Location is one of the most important factors when selecting a solar system because the same solar desalination systems will provide higher water production rate at location with higher solar radiation thus lowering the overall water cost [256,257].

3.3.1. Comparison of solar systems

In order to better select the processes, the advantages and disadvantages of solar systems used for indirect solar desalination are listed in Table 16. As for the direct solar desalination, a general rule of thumb for simple solar stills is 3–5 l of water/day/m^2 [257]. For example, for a small family that consumes water at a rate of about 0.6 m^3/d [242], 120–200 m^2 land area is needed if a simple solar still is used, the area might be doubled if one considers the spacing between the solar still systems, which implies that this may not be a realistic application because of the large area needed.

3.3.2. Concentrated solar power (CSP) VS PV

CSP and PV are the two most studied solar technologies used for seawater desalinations [80]. A CSP plant combined with an RO system is regarded as one of the best choices for solar desalination [154]. Between PV and CSP, CSP has the advantage of using a thermal storage system for longer hours of operation after sunset

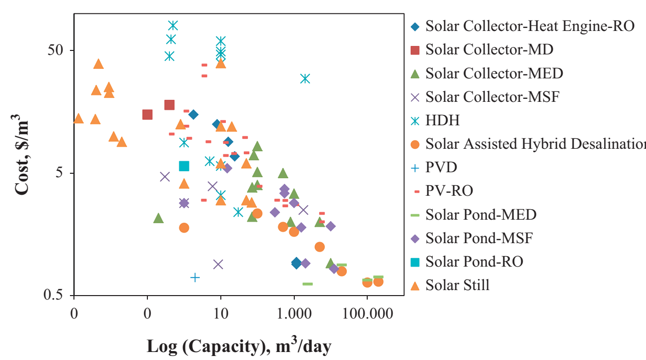

Fig. 20. Solar desalination capacities vs. cost (the source data and the references for the points is shown in Table A1).

Table 16
Comparison of different solar systems.

	PV	Solar pond	Flat collector	Concentrating collector
Resource	GHI	GHI	GHI	DNI
Humidity	Tolerable	Tolerable	Tolerable	Not tolerable
Dry areas	GHI: less sensitive to dust	GHI: less sensitive to dust	GHI: less sensitive to dust	DNI: very sensitive to dust
Land available	Easier to find	More difficult	Easier to find	More difficult
Type of land	Light slopes tolerated	Flat	Light Slope tolerated	Flat
Water	Not needed	Needed	Needed	Needed
Connection to the grid	Low or medium voltage	Low or medium voltage	Low or medium voltage	Medium or high voltage
Complexity	Low number of different equipment	Low number of different equipment	Several different equipment	Several different equipment
Construction	Simple, quick and flexible	Simple, quick	Longer and complex	Longer and complex
Scalability	small, medium, large scale	small scale	small and medium scale	large scale
O&M	Simple, some staff at site	Skillful operator needed	Skillful operator needed	Complex and skilled team
Type of production	Distributed/central generation	Distributed	Distributed	Central generation
Storage	Battery	None	Battery or cheap thermal storage	High temperature thermal storage
Output stability	Not stable, depends on irradiation	Relative stable	Relative stable with thermal storage	Relative stable with thermal storage
Thermal plants integration	No	No	No	Yes
Number of developers	Many	NA	Many	Few

Table A1
Cost table.

Ref.	Cost ($)	Configuration	Capacity (m^3/d)	Notes
[143,261]	15	ETC+ORC+RO	1.8	Study carried out through Agriculture University of Athens, Greece, authors' design radiation 1000 W/m^2. Based on location Athens, GHI 4.58 kW h/m^2/d
[142]	9	ETC+ORC+RO	16	Study carried out through Agriculture University of Athens, Greece, authors' design radiation 1000 W/m^2
[143,158]	12.5	ETC–ORC–RO	8	Study carried out through Agriculture University of Athens, Greece, authors' design radiation 1000 W/m^2
[142,144,159]	6.85	ETC-Cascade ORC–RO	24	Study carried out through Agriculture University of Athens, Greece, authors' design radiation 1000 W/m^2
[124]	10.4	PV–RO	0.4	PV panels working at solar irradiance of the half value of that of the test conditions (1000 W/m^2) by Agriculture University of Athens, Greece, reported cost €7.8/m^3 water, PV capacity 0.85kW
[126]	6.95	PV–RO	12	PV capacity 30.22 kW, design solar radiation 1000 W/m2, two wind turbines and 40% PV has the lowest water production cost (€ 5.21/m3).
[126]	8.88	PV–RO	12	3096 m^3/year production with 100% PV driven, cost €6.64/m^3 fresh water, design solar radiation 1000 W/m^2, PV capacity 13.2 kW
[140]	0.94	FPC–ORC–RO	1,166	Design points 850 W/m^2, Based on the studied location, NASA GHI data 5.69 kW h/m^2/d
[140]	0.93	CPC–ORC–RO	1,166	Design points 850 W/m^2, Based on the studied location, DNI is 7.01 kW h/m^2/d
[140]	0.90	PTC–ORC–RO	1,166	Design points 850 W/m^2, Based on the studied location, DNI is 7.01 kW h/m^2/d
[80,233]	15	FPC–PV–MD	0.1	Location: Aqaba port, Jordan; GHI 5.891 kW h/m^2/d
[233]	18	Flat Collector–MD	0.4	Location: Aqaba port, Jordan; GHI 5.891 kW h/m^2/d
[79]	2.15–4.70	FPC–MED	0.2	Location: Richmond, California, Jordan; GHI 4.571 kW h/m^2/d
[106]	2.2–4.7	PTC–MED	72	Experimental, Convert to dollar using 192.21 Spain Pesetas per United States Dollar; Based on the studied location, DNI is 5.601 kW h/m^2/d
[82]	4	FPC–MED	100	Experiments at Sydney, GHI is 4.981 kW h/m^2/d
[82]	5.1	ETC–MED	100	Experiments at Sydney, GHI is 4.981 kW h/m^2/d
[67,82]	5–6.7	ETC–MED	500	Location: Abu Dhabi, GHI is 5.611 kW h/m^2/d
[67,80]	8.3–9.3	ETC–MED	100	Location: Abu Dhabi, GHI is 5.611 kW h/m^2/d
[67,80]	3.4–4.4	ETC–MED	1,000	Location: Abu Dhabi, GHI is 5.611 kW h/m^2/d
[81]	7–10	ETC–MED	80	Experiments; Location: Abu Dhabi, GHI is 5.611 kW h/m^2/d
[80,107,273]	2	PTC–MED	800	Based on studied location in Spain, DNI is estimated as 5.601 kW h/m^2/d
[107]	3.82–4.93	PTC–MED	72	Based on studied location in Spain, DNI is estimated as 5.601 kW h/m^2/d
[70]	0.92	Collector–MED	10,000	Based on studied location: Eilat, Israel, NASA data showed GHI 5.65 kW h/m^2/d
[128]	2	solar thermal collector - MED	5,000	Annual insulation was 2000 kW h/m^2, peak radiation was 1000 W/m^2
[42]	0.9	FPC–MSF	8.5	Experiments at Tamilnadu, India, location, author mentioned 400–900 W/m^2
[39]	4.67	FPC–MSF	0.3	Based on studied location in Tianjin, China, GHI is estimated as 4.36 kW h/m^2/d from NASA database
[39]	3.9	FPC–MSF	6	Based on studied location in Tianjin, China, GHI is estimated as 4.36 kW h/m^2/d from NASA database
[37]	2.5–3.8	PTC–MSF	1,800–3,000	Studied location: SE Spain, estimated DNI from NASA database is 5.6 kW h/m^2/d
[233]	2.84	Collector-MSF	1	Authors were in Kuwait where has GHI about 5.40 kW h/m^2/d
[274]	3.3	HDH	10	
[274]	2.4	HDH	30	
[82,275,276]	29.46	HDH	2,000	Location: South Tunisia, which has GHI about 5.24 kW h/m^2/d
[277]	8.87	FPC–CAOW HDH	1	A demonstration system was installed and commissioned in Jeddah/Kingdom of Saudi-Arabia
[277]	6.25	FPC–CAOW HDH	5	Assume in Jeddah/Saudi Arabia
[277]	5.71	FPC–CAOW HDH	10	Assume in Jeddah/Saudi Arabia
[207]	45	FPC–HDH	0.4	Location: Sfax in Tunisia. Based on NASA database, GHI is estimated about 4.87 kW h/m^2/d
[207]	80	FPC–HDH	0.5	Location: Sfax in Tunisia. Based on NASA database, GHI is estimated about 4.87 kW h/m^2/d
[275]	61.65–109.6	HDH	0.44–0.5	Location: Sfax in Tunisia. Based on NASA database, GHI is estimated about 4.87 kW h/m^2/d
[275]	39.25	FPC–CAOW HDH	10	Location: Tunisian, Solar radiation 510 W/m^2
[275]	59.6	FPC–CAOW HDH	10	Location: Tunisian, Solar radiation 510 W/m^2
[275]	49.05	FPC–CAOW HDH	10	Location: Tunisian, Solar radiation 510 W/m^2
[275]	46.31	FPC–CAOW HDH	10	Location: Tunisian, Solar radiation 510 W/m^2
[106]	2.34	Hybrid–MED–HP	100	Model only, cost information by converting to dollar using 192.21 Spain Pesetas per United States Dollar. Based on studied location, using NASA database one could estimate GHI about 4.65 kW h/m^2/d
[106]	1.82	Hybrid–MED–HP	500	Model only, cost information by converting to dollar using 192.21 Spain Pesetas per United States Dollar. Based on studied location, using NASA database one could estimate GHI about 4.65 kW h/m^2/d
[106]	1.66	Hybrid–MED–HP	1,000	Model only, cost information by converting to dollar using 192.21 Spain Pesetas per United States Dollar. Based on studied location, using NASA database one could estimate GHI about 4.65 kW h/m^2/d
[106]	1.25	Hybrid–MED–HP	5,000	Model only, cost information by converting to dollar using 192.21 Spain Pesetas per United States Dollar. Based on studied location, using NASA database one could estimate GHI about 4.65 kW h/m^2/d
[70]	0.64	Hybrid–MED	100,000	Location: Zikim, Israel; Based on studied locations, readers could use NASA database and estimate GHI close to 5.57 kW h/m^2/d
[60]	0.79	Hybrid–SP–MED/RO	20,000	paper used 2000 kW h/m^2 annual solar insulation, authors location is Tel Aviv, Israel
[60]	0.65	Hybrid–SP–MED/RO	200,000	paper used 2000 kW h/m^2 annual solar insulation, authors location is Tel Aviv, Israel
[28,82]	1.79	Hybrid–SP–MSF	1	Based on studied location, Safat in Kuwait, readers could estimate GHI about 5.4 kW h/m^2/d from NASA database
[177]	1	PVD	0.013	Monthly average daily global solar radiation in Bahrain 3000–7200 W/m^2/d. Location: Isatown, Bahrain
[177]	0.702	PVD	0.1	Monthly average daily global solar radiation in Bahrain 3000–7200 W/m^2/d. Location: Isatown, Bahrain
[106]	3.9	PV–RO	100	Model only, cost information by converting to dollar using 192.21 Spain Pesetas per United States Dollar. Based on studied location, using NASA database one could estimate GHI about 4.65 kW h/m^2/d
[106]	2.99	PV–RO	500	

Table A1 (*continued*)

Ref.	Cost ($)	Configuration	Capacity (m^3/d)	Notes
				Model only, cost information by converting to dollar using 192.21 Spain Pesetas per United States Dollar. Based on studied location, using NASA database one could estimate GHI about 4.65 kW h/m^2/d
[106]	2.76	PV–RO	1,000	Model only, cost information by converting to dollar using 192.21 Spain Pesetas per United States Dollar. Based on studied location, using NASA database one could estimate GHI about 4.65 kW h/m^2/d
[106]	2.34	PV–RO	5,000	Model only, cost information by converting to dollar using 192.21 Spain Pesetas per United States Dollar. Based on studied location, using NASA database one could estimate GHI about 4.65 kW h/m^2/d
[80,133]	31	PV–RO	3.1	PV capacity was 4 kW, study carried out by CRES, Laviro in Greece; water production is 130 l h with energy recovery system for RO unit, reported cost €23/m^3 water. Based on studied location, readers could use NASA database to estimate GHI as 4.95 kW h/m^2/d
[80]	9.75	PV–RO	40	
[278,279]	9	PV–RO	4	Yearly solar insulation was 2000 kW h/m^2
[280]	16	PV–RO	1	A small reverse osmosis (RO) plant supplied by a photovoltaic (PV) power supply has been installed at the island of Gran Canada. Based on studied location, readers could estimate GHI close to 5.67 kW h/m^2/d
[281]	38–42	PV–RO	3.1–4.6	Studied location Tan Tan City, Moroca, solar insulation 4624 W h/m^2, desalination system operated 2434 h/year with a lifetime of 20 years for the equipment is considered. The analysis was made assuming 3% and 5% rate of return and a yearly water production of 1350 m^3. A total water cost of €29/m^3 of fresh water for a rate of return of 3% is calculated while a total water cost of around €32/m^3 is calculated for 5% annual rate of return.
[128]	2	PV–RO	5,000	Annual solar energy 2000 kW h/m^2
[132]	7.21	PV–RO	20	PV capacity 11.25 kW, the system is a diesel assisted system. Location is Abu Dhabi. Based on studied location, readers could estimate GHI close to 5.61 kW h/m^2/d
[132]	7.3	PV–RO	44	PV capacity 22.49 kW 100% driven by solar energy. Location is Abu Dhabi. Based on studied location, readers could estimate GHI close to 5.61 kW h/m^2/d
[134]	13.16	PV–RO	10	PV capacity 4.8kW, location is ITC–DESSOL, Gran Canaria, Spain, based on studied location, readers could estimate GHI from NASA as 5.4 kW h/m^2/d
[80,135,136]	3	PV–RO	3	Location at Loughborough University, UK. PV system has solar tracking system. Location GHI could be estimated as 2.65 kW h/m^2/d
[137]	9.6	PV–RO	1.2	PV capacity 4.8 kW; location is CIEA-ITC, Canary Islands, Spain; Based on studied location, one could estimate GHI close to 5.4 kW h/m2/d based on NASA data
[139]	3	PV–RO	300	PV capacity 50kW; Location was GECOL at Ras Ejder, Libya. Based on studied location, solar radiation could estimate as 5.24 kW h/m^2/d
[233]	2.7	PV–RO	500	Annual insulation as 2000 kW h/m^2, design radiation was 1000W/m^2
[233]	12.05	PV–RO	1	Location: Safat in Kuwait; using NASA database to estimate GHI 5.4 kW h/m^2/d
[82]	0.67–1.44	SP–MED	100,000	Annual solar insulation 2400 kW h/m^2/y.
[60]	0.89	SP–MED	20,000	Authors used 2000 kW h/m^2 annual insulation; authors location was Tel Aviv, Israel
[60]	0.71	SP–MED	200,000	Authors used 2000 kW h/m^2 annual insulation; authors location was Tel Aviv, Israel
[25]	0.621	SP–MED	2,348	30 MW gas engine waste heat was discharged into solar pond. Solar pond size 7800 m^2; If authors location was used, the GHI could be estimated as 4.54 kW h/m^2/d
[25]	0.466	SP–MED	15,044	120 MW gas engine waste heat was discharged into solar pond. Solar pond size 7800 m^2; If authors location was used, the GHI could be estimated as 4.54 kW h/m^2/d
[28]	2.84	SP–MSF	1	Paper reported 1.63 KD per cubic meter water cost, authors used 1 KD=$3.4; location: Safat, Kuwait where NASA database shows GHI as 5.40 kW h/m^2/d
[28]	5.7	SP–RO	1	Paper reported 1.63 KD per cubic meter water cost, authors used 1 KD=$3.4; location: Safat, Kuwait where NASA database shows GHI as 5.40 kW h/m^2/d
[23]	5.48	SP–MSF	15	Location: Tan Tan City, Moroca where NASA database showed GHI 5.75 kW h/m^2/d; Solar pond size 2500 m^2
[23]	2.39	SP–MSF	300	Location: Tan Tan City, Moroca where NASA database showed GHI 5.75 kW h/m^2/d; Solar pond size36,000 m^2
[24]	2.85	SP–MSF	1,000	Pond size 80,000 m^2. Based on studied location, check NASA database and estimated DNI as 6 kW h/m^2/d
[24]	1.84	SP–MSF	10,000	Pond size 80,000 m^2. Based on studied location, check NASA database and estimated DNI as 6 kW h/m^2/d
[25]	0.916	SP–MSF	2,040	30 MW gas engine waste heat was discharged into solar pond. Solar pond size 7800 m^2; If authors location was used, the GHI could be estimated as 4.54 kW h/m^2/d
[25]	0.827	SP–MSF	12,378	120 MW gas engine waste heat was discharged into solar pond. Solar pond size 7800 m^2; If authors location was used, the GHI could be estimated as 4.54 kW h/m^2/d
[26]	1.8	SP–MSF	1,570	Pond size 70,000 m^2, radiation less than <350 W/m^2
[22]	3.71	SP–MSF	550	The author listed location but chose data from Dakar due to lacking of solar data; pond size 65,361 m^2; solar insulation: 246.3 W/m^2
[22]	3.42	SP–MSF	550	The author listed location but chose data from Dakar due to lacking of solar data; pond size49,441 m^2; solar insulation: 246.3 W/m^2
[282]	2.88	ST	70	
[82,275]	4.11	ST	1–50	
[82,283]	3	ST	10	
[82,283]	6	ST	10	
[82,283]	12	ST	10	
[82,283]	3	ST	50	
[82,283]	6	ST	50	
[82]	23.8	FPC–ST	0.004	
[82]	9.95	Multi-effect ST	0.012	
[82]	9	Multi-effect ST	0.02	
[82,275]	39.456	Multi-effect ST	10	
[82,275]	11.99	ST	20	Location: Sydney where NASA database showed GHI 4.98 kW h/m^2/d
[28,233]	12.5	ST	0.8	Location: Safat, Kuwait where NASA database showed GHI 5.4 kW h/m^2/d
[284]	25.2	Single-slope ST	0.00888	Design solar insulation 850 W/m^2. Based on studied location, NASA database showed GHI 5.35 kW h/m^2/d
[284]	14	Single-slope ST	0.00132	Design solar insulation 800 W/m^2. Based on studied location, NASA database showed GHI 5.05 kW h/m^2/d
[284]	39		0.00463	Design solar insulation 850 W/m^2. Based on studied location, NASA database showed GHI 3.35 kW h/m^2/d

Table A1 (*continued*)

Ref.	Cost ($)	Configuration	Capacity (m^3/d)	Notes
		ST with solar collector		
[284]	13.8	ST with solar concentrator	0.0038	Design solar insulation 800 W/m^2. Based on studied location, NASA database showed GHI 5.35 kW h/m^2/d
[284]	22.6	ST using pyramid-shaped	0.009	Design solar insulation 800 W/m^2. Based on studied location, NASA database showed GHI 5.05 kW h/m^2/d

1. For capacity range, use low end, i.e., 7–10 m^3/d, choose 7 m^3/d.
2. For cost range, pick middle cost, i.e., 7–10 \$/m^3, use low cost due to the technology development and solar products price drop.
3. Convert all the currency into dollars based on Oct.14, 2011 currency rate.
4. If hourly rate is given, convert to daily production using 8 h, i.e., 3 m^3/h, converted as 24 m^3/d (except authors directly mentioned operation hours and daily production).
5 For research given by L/year, convert to daily production by dividing 365.
6. FPC, ETC, CPC and PTC combined with desalination system just generalized as collector+desalination, i.e., FPC+RO is called collector+RO in cost figure.
7. Single effect solar still, multi-effect solar still and collector/PV combined with solar still are all abbreviated as ST.
8. All kinds of power cycles are all called used engine in Figures, i.e., FPC with ORC driven RO used collector-engine-RO to represent in figure.
9. Different HDH process are generalize called HDH process, for example, FPC+CAOW HDH process is represented as HDH only.
10. GHI: NASA 22-year monthly and annual average showed Insolation Incident on a horizontal surface, unit kW h/m^2/d. Data is estimated based on authors studied location and check NASA database.
11. DNI: Based on the studied location, NASA 22-year monthly and annual average data showed direct normal radiation, unit is kW h/m^2/d, and Data is estimated based on authors studied location and check NASA database.

and the ability to use a backup fuel for unexpected conditions[262]. CSP is regarded as the appropriate solar power technology for multi-megawatt scale [263]. However, on a cloudy or foggy day, the DNI could be negligible and CSP plants would have little output. Therefore heat storage is a very important issue for CSP. New concepts on phase change materials tailored for CSP applications are presently under active research and development. In practice, DNI of 1900 kW h/m^2/year to 2100 kW h/m^2/year is treated as the threshold for CSP [264]. Below that, other solar electric technologies that take advantage of both direct and diffuse irradiance, such as photovoltaics, may have some advantages [264]. Besides, areas close to the sea could have higher humidity and therefore affect the DNI. In addition, coastal areas normally have higher land value, either tourist areas or high population density [265], while CSP requires large, flat land which could increase the cost of CSP assisted desalination plants.

3.3.3. PV assisted desalination

PV could be used to power a RO or MVC system which only use mechanical energy. The retail price for PV modules makesthe solar sub-unit cost a key factor in the economic feasibility of PV–RO desalination [266]. In recent years, PV priceshave dropped dramatically. PVs' modular design allowsa PV plant to be relatively easy to scale up so as to allow a project to be built in phases. PV operation does not need water at all, the PV–RO systems are two systems developed independently. However, if the local community already has a de-centralized power generation system, i.e., diesel or natural gas small scale power generation system, PV could not make use of the existing system like a CSP based system which could be easily integrated with a fossil fuel based power system. Furthermore, RO desalination requires strigent pretreatment which normally needs skillful labor. Therefore in remote areas where it is hard to find skillful operators and where both energy and water are precious, the application of the PV driven desalination system still needs to be carefully evaluated.

3.4. Desalination capacity effects

Reducing cost is the key driving force for considering solar desalination. Desalination cost is affected by many factors including solar system location, solar radiation, desalination system energy efficiency, etc., as previous discussed. In addition to the above, the desalination system capacity has a direct impact on the water cost, as illustrated in Fig. 20, which lists the reported solar desalination systems with cost informaiton. The souce data for this figure is presented in the Appendix Table A1.

From Fig. 20, it is clear that larger capacity of solar desalination plants will lead to lower water cost. And it can be seen that hybrid plants and solar pond driven desalinaton plants generally have relative lower unit water cost compared to other type of solar desalination systems when the capacities are similar. In addtion, most very small capacity (<0.1 m^3/d) solar desalination systems with reported cost are solar still systems while most large scale (>1000 m^3/d) solar desalination systems with unit water cost infomration are either hybrid or solar driven thermal process; information is available ononly 3 PVD and solar MD solar assisted seawater desalination systems and more studies are needed to arrive at meaningful cost conclusions; For small (0.1–100 m^3/d) and medium (100–1000 m^3/d) capacities, there is no clear evidence on which combinations are better, which means the configuration selection must be made on a case by case basis, keeping in mind that optimization is a complex problem [267].

3.5. Cogeneration and process using low grade heat

Considerable research focuses on using solar desalination in remote, arid areas, which normally use small scale desalination systems. Fig. 20 shows that hybrid thermal systems generally have a relatively lower cost as compared with similar capacity solar only desalination systems, however, most of them have capacities larger than 100 m^3/d. For places far away from the power grid and water system, not only water is needed but also power is needed [268]. Small desalination systems using waste heat from decentralized diesel generators, decentralized small scale natural gas engines or geothermal energy could achieve lower cost especialy if solar is the only power supply systems [141]. Therefore, it is very important to study small scale hybrid desalination systems. On one hand, the hybrid system could reduce the fossil fuel energy concumption and save fuel transporation costs, on the other hand, hybrid systems could provide low water cost and avoid the drawback of an intermittent solar source and provide crucial water that is not weather and season dependent. However, not many studies have been reported on small scale solar assisted hybrid desalination systems. In addition, heat energy from solar collectors is not really the same as

heat energy from waste heat. Waste heat sources are considered as "once through" heat sources as opposed to the solar resource being a re-circulating source. This difference could impact the choice of heat engines for the desalination system. Therefore, the two types of heat sources should be analyzed separately and cannot be assumed that conclusions for solar thermal are valid for hybrid desalination or waste heat usage applications [269,291,292].

4. Outlook and conclusions

Compared with conventional water treatment processes, desalination is an energy intensive process. Solar resources are abundant and could be used for desalination applications, whose technical feasibility has already been proved. Most current solar desalination systems are two independent systems solar and desalination combined together, which are still relatively expensive and depend on location, weather and season. Current research shows that solar/fossil/desalination hybrid systems are more economical and could overcome the intermittence of solar energy. Additional research is needed on solar/fossil fuel hybrid systems, especially waste heat from decentralized thermal power systems for water and power cogeneration because both are crucial in remote areas. In order to reduce fuel consumption and overcome the intermittence of the solar source, waste heat from decentralized systems could be used. However, any waste heat source or solar thermal heat source should be analyzed separately and cannot assume that the conclusions for solar thermal are the same as for hybrid desalination or waste heat usage applications. With the cost reduction of future solar systems and the development of novel solar technologies as well as accurate solar radiation data collection and modeling [270–272], solar desalination could be a valid option for future desalination plants.

Acknowledgments

The research leading to this paper was funded by the State of Florida through the Florida Energy Systems Consortium (FESC) funds. The authors also thank researchers from GE Global Research Center for their kindly help and discussions about the paper.

References

[1] Service RF. Desalination freshens up. Science 2006;313:1088–90.
[2] Shannon MA, Bohn PW, Elimelech M, Georgiadis JG, Marinas BJ, Mayes AM. Science and technology for water purification in the coming decades. Nature 2008;452:301–10.
[3] Schiermeier Q. Water: purification with a pinch of salt. Nature 2008;452:260–1.
[4] Population Reference Bureau. World population highlights: key findings from PRB'S 2010. World Population Data Sheet 2010;65(2) July.
[5] Mehanna M, Saito T, Yan J, Hickner M, Cao X, Huang X, et al. Using microbial desalination cells to reduce water salinity prior to reverse osmosis. Energy & Environmental Science 2010;3:1114.
[6] Bajpayee A, Luo T, Muto A, Chen G. Very low temperature membrane-free desalination by directional solvent extraction. Energy & Environmental Science 2011;4:1672.
[7] Hoffman AR. Water security: a growing crisis and the link to energy. AIP Conference Proceedings 2008;1044:55–63.
[8] The IDA Desalination Yearbook 2011–2012 | Water desalination report.
[9] Kalogirou SA. Seawater desalination using renewable energy sources. Progress in Energy and Combustion Science 2005;31:242–81.
[10] Arjunan TV, Aybar HS, Nedunchezhian N. Status of solar desalination in India. Renewable and Sustainable Energy Reviews 2009;13:2408–18.
[11] Jacobson MZ. Review of solutions to global warming, air pollution, and energy security. Energy & Environmental Science 2009;2:148.
[12] Blanco J, Malato S, Fernández-Ibañez P, Alarcón D, Gernjak W, Maldonado MI. Review of feasible solar energy applications to water processes. Renewable and Sustainable Energy Reviews 2009;13:1437–45.
[13] Cho A. Energy's tricky tradeoffs. Science 2010;329:786–7.
[14] Mussati S, Aguirre P, Scenna NJ. Optimal MSF plant design. Desalination 2001;138:341–7.
[15] Mussati SF, Aguirre PA, Scenna NJ. Improving the efficiency of the MSF once through (MSF-OT) and MSF-mixer (MSF-M) evaporators. Desalination 2004;166:141–51.
[16] Ali E. Understanding the operation of industrial MSF plants Part I: Stability and steady-state analysis. Desalination 2002;143:53–72.
[17] Ali E. Understanding the operation of industrial MSF plants Part II: Optimization and dynamic analysis. Desalination 2002;143:73–91.
[18] Cardona E, Piacentino A. Optimal design of cogeneration plants for seawater desalination. Desalination 2004;166:411–26.
[19] de Gunzbourg J, Larger D. Cogeneration applied to very high efficiency thermal seawater desalination plants. Desalination 1999;125:203–8.
[20] Darwish MA, Alsairafi A. Technical comparison between TVC/MEB and MSF. Desalination 2004;170:223–39.
[21] Micale G, Rizzuti L, Cipollina A. Seawater desalination conventional and renewable energy processes. Springer Link; 2009.
[22] Engineering studyof desalination using salt gradient solar ponds. Agency for international development; 1981.
[23] Szacsvay T, Hofer-Noser P, Posnansky M. Technical and economic aspects of small-scale solar-pond-powered seawater desalination systems. Desalination 1999;122:185–93.
[24] Posnansky M. Technical and economical aspects of solar desalination with particular emphasis on solar pond powered distillation plants. Desalination 1987;67:81–95.
[25] Safi MJ, Korchani A. Cogeneration applied to water desalination: Simulation of different technologies. Desalination 1999;125:223–9.
[26] Agha KR. The thermal characteristics and economic analysis of a solar pond coupled low temperature multi stage desalination plant. Solar Energy 2009;83:501–10.
[27] Lu H, Walton JC, Hein H. Thermal desalination using MEMS and salinity-gradient solar pond technology. U.S. Department of the Interior, Bureau of Reclamation. : 2002.
[28] Suri RK, Al-Marafie AMR, Al-Homoud AA, Maheshwari GP. Cost-effectiveness of solar water production. Desalination 1989;71:165–75.
[29] Tahri K. The prospects of fresh water supply for Tan Tan city from non-conventional water resources. Desalination 2001;135:43–50.
[30] Hayes DWJ, Kipps JAL. Salt-gradient solar ponds from concentrated subsurface agricultural drainage waters of the San Joaquin Valley, California. Desalination 1992;88:301–9.
[31] Lu H, Swift AHP, Hein J, Walton JC. Advancements in salinity gradient solar pond technology based on sixteen years of operational experience. Journal of Solar Energy Engineering 2004;126:759–67.
[32] Velmurugan V, Srithar K. Prospects and scopes of solar pond: a detailed review. Renewable and Sustainable Energy Reviews 2008;12:2253–63.
[33] Trieb F, Müller-Steinhagen H. Concentrating solar power for seawater desalination in the Middle East and North Africa. Desalination 2008;220:165–83.
[34] Kalogirou S. The potential of solar industrial process heat applications. Applied Energy 2003;76:337–61.
[35] García IL, Álvarez JL, Blanco D. Performance model for parabolic trough solar thermal power plants with thermal storage: comparison to operating plant data. Solar Energy 2011;85:2443–60.
[36] Shaobo H, Zhang Z, Huang Z, Xie A. Performance optimization of solar multi-stage flash desalination process using pinch technology. Desalination 2008;220:524–30.
[37] García-Rodríguez L, Gómez-Camacho C. Conditions for economical benefits of the use of solar energy in multi-stage flash distillation. Desalination 1999;125:133–8.
[38] García-Rodríguez L, Gómez-Camacho C. Thermoeconomic analysis of a solar parabolic trough collector distillation plant. Desalination 1999;122: 215–24.
[39] Jiang J, Tian H, Cui M, Liu L. Proof-of-concept study of an integrated solar desalination system. Renewable Energy 2009;34:2798–802.
[40] Abu-Jabal MS, Kamiya I, Narasaki Y. Proving test for a solar-powered desalination system in Gaza-Palestine. Desalination 2001;137:1–6.
[41] Farwati MA. Theoretical study of multi-stage flash distillation using solar energy. Energy 1997;22:1–5.
[42] Joseph J, Saravanan R, Renganarayanan S. Studies on a single-stage solar desalination system for domestic applications. Desalination 2005;173: 77–82.
[43] Nafey AS, Mohamad MA, El-Helaby SO, Sharaf MA. Theoretical and experimental study of a small unit for solar desalination using flashing process. Energy Conversion and Management 2007;48:528–38.
[44] Kalogirou S. Survey of solar desalination systems and system selection. Energy 1997;22:69–81.
[45] Raach H, Mitrovic J. Simulation of heat and mass transfer in a multi-effect distillation plant for seawater desalination. Desalination 2007;204:416–22.
[46] Slesarenko VN. Comparison of the efficiency of MSF and thin-film desalination plants. Desalination 2003;158:295–302.
[47] Kronenberg G. Cogeneration with the LT-MED desalination process. Desalination 1997;108:287–94.

[48] Slesarenko VV. Heat pumps as a source of heat energy for desalination of seawater. Desalination 2001;139:405–10.
[49] Al-Juwayhel F, El-Dessouky H, Ettouney H. Analysis of single-effect evaporator desalination systems combined with vapor compression heat pumps. Desalination 1997;114:253–75.
[50] Alarcón-Padilla DC, García-Rodríguez L, Blanco-Gálvez J. Experimental assessment of connection of an absorption heat pump to a multi-effect distillation unit. Desalination 2010;250:500–5.
[51] Ophir A, Lokiec F. Advanced MED process for most economical sea water desalination. Desalination 2005;182:187–98.
[52] Sommarva C. Utilisation of power plant waste heat steams to enhance efficiency in thermal desalination. Desalination 2008;222:592–5.
[53] Al Hawaj O, Darwish MA. A solar pond assisted multi-effect desalting system. Desalination 1994;99:119–35.
[54] Garman MA, Muntasser MA. Sizing and thermal study of salinity gradient solar ponds connecting with the MED desalination unit. Desalination 2008;222:689–95.
[55] Lu H, C, Walton J, HP, Swift A. Desalination coupled with salinity-gradient solar ponds. Desalination 2001;136:13–23.
[56] Tsilingiris PT. The analysis and performance of large-scale stand-alone solar desalination plants. Desalination 1995;103:249–55.
[57] Caruso G, Naviglio A. A desalination plant using solar heat as a heat supply, not affecting the environment with chemicals. Desalination 1999;122:225–34.
[58] Caruso G, Naviglio A, Principi P, Ruffini E. High-energy efficiency desalination project using a full titanium desalination unit and a solar pond as the heat supply. Desalination 2001;136:199–212.
[59] Leblanc J, Andrews J, Akbarzadeh A. Low-temperature solar-thermal multi-effect evaporation desalination systems. International Journal of Energy Research 2010;34:2151–7.
[60] PG. Potential uses of solar energy for seawater desalination. Desalination 1995;101:11–20.
[61] Daniel H. The application of solar energy for large-scale seawater desalination. Desalination 1992;89:115–83.
[62] El-Nashar AM. An optimal design of a solar desalination plant. Desalination 1993;93:597–614.
[63] El-Nashar AM. Validating the performance simulation program SOLDES using data from an operating solar desalination plant. Desalination 2000;130:235–53.
[64] El-Nashar AM. Predicting part load performance of small MED evaporators—a simple simulation program and its experimental verification. Desalination 2000;130:217–34.
[65] El-Nashar AM. Optimizing the operating parameters of a solar desalination plant. Solar Energy 1992;48:207–13.
[66] El-Nashar AM. Seasonal effect of dust deposition on a field of evacuated tube collectors on the performance of a solar desalination plant. Desalination 2009;239:66–81.
[67] El-Nashar AM. The economic feasibility of small solar MED seawater desalination plants for remote arid areas. Desalination 2001;134:173–86.
[68] El-Nashar AM. Economics of small solar-assisted multiple-effect stack distillation plants. Desalination 2000;130:201–15.
[69] Kalogirou S. Economic analysis of a solar assisted desalination system. Renewable Energy 1997;12:351–67.
[70] Sagie D, Feinerman E, Aharoni E. Potential of solar desalination in Israel and in its close vicinity. Desalination 2001;139:21–33.
[71] Zarza E, Ajona J, León J, Gregorzewski A, Genthner K. Solar thermal desalination project at the Plataforma Solar de Almeria. Solar Energy Materials 1991;24:608–22.
[72] Aly NH, El-Figi AK. Mechanical vapor compression desalination systems—a case study. Desalination 2003;158:143–50.
[73] Siqueiros J, Holland FA. Water desalination using heat pumps. Energy 2000;25:717–29.
[74] Ji JG, Wang RZ, Li LX, Ni H. Simulation and analysis of a single-effect thermal vapor-compression desalination system at variable operation conditions. Chemical Engineering and Technology 2007;30:1633–41.
[75] Nafey AS, Fath HES, Mabrouk AA. Thermoeconomic design of a multi-effect evaporation mechanical vapor compression (MEE-MVC) desalination process. Desalination 2008;230:1–15.
[76] El-Sayed YM. Thermoeconomics of some options of large mechanical vapor-compression units. Desalination 1999;125:251–7.
[77] Darwish MA. Thermal analysis of vapor compression desalination system. Desalination 1988;69:275–95.
[78] Amer AOB. Development and optimization of ME-TVC desalination system. Desalination 2009;249:1315–31.
[79] Badawi WT. Optimal water cost from solar-powered multieffect distillation. Desalination 1983;44:153–65.
[80] Ali MT, Fath HES, Armstrong PR. A comprehensive techno-economical review of indirect solar desalination. Renewable and Sustainable Energy Reviews 2011;15:4187–99.
[81] El-Nashar AM, Samad M The solar desalination plant in Abu Dhabi: 13 years of performance and operation history. Renewable Energy, May;14:263–274.
[82] Al-Hallaj S, Parekh S, Farid MM, Selman JR. Solar desalination with humidification–dehumidification cycle: review of economics. Desalination 2006;195:169–86.
[83] Blanco J, AlarcóN D. The PSA experience on solar desalination: technology development and research activities. In: Rizzuti L, Ettouney HM, Cipollina A, editors. Solar desalination for the 21st century, Dordrecht: Springer The Netherlands; p. 195–206.
[84] Wang Y, Lior N. Performance analysis of combined humidified gas turbine power generation and multi-effect thermal vapor compression desalination systems—Part 1: The desalination unit and its combination with a steam-injected gas turbine power system. Desalination 2006;196:84–104.
[85] Wang Y, Lior N. Performance analysis of combined humidified gas turbine power generation and multi-effect thermal vapor compression desalination systems Part 2: The evaporative gas turbine based system and some discussions. Desalination 2007;207:243–56.
[86] Ansari K, Sayyaadi H, Amidpour M. A comprehensive approach in optimization of a dual nuclear power and desalination system. Desalination 2011;269:25–34.
[87] Kouhikamali RMM. Process investigation of different locations of thermo-compressor suction in MED–TVC plants. Desalination 2011;280:134–8.
[88] Zimerman Z. Development of large capacity high efficiency mechanical vapor compression (MVC) units. Desalination 1994;96:51–8.
[89] Ettouney H. Design of single-effect mechanical vapor compression. Desalination 2006;190:1–15.
[90] Marcovecchio M, Aguirre P, Scenna N, Mussati S. Global optimal design of mechanical vapor compression (MVC) desalination process. 20th European symposium on computer aided process engineering, 2010; 28: p. 1261–1266.
[91] Bahar R, Hawlader MNA, Woei LS. Performance evaluation of a mechanical vapor compression desalination system. Desalination 2004;166:123–7.
[92] Slesarenko VV. Desalination plant with absorption heat pump for power station. Desalination 1999;126:281–5.
[93] Wang Y, Lior N. Proposal and analysis of a high-efficiency combined desalination and refrigeration system based on the LiBr–H_2O absorption cycle—Part 1: System configuration and mathematical model. Energy Conversion and Management 2011;52:220–7.
[94] Wang Y, Lior N. Proposal and analysis of a high-efficiency combined desalination and refrigeration system based on the LiBr–H_2O absorption cycle—Part 2: Thermal performance analysis and discussions. Energy Conversion and Management 2011;52:228–35.
[95] Mandani F, Ettouney H, El-Dessouky H. LiBr–H_2O absorption heat pump for single-effect evaporation desalination process. Desalination 2000;128:161–76.
[96] Gomri R. Thermal seawater desalination: possibilities of using single effect and double effect absorption heat transformer systems. Desalination 2010;253:112–8.
[97] Al-Ansari A, Ettouney H, El-Dessouky H. Water–zeolite adsorption heat pump combined with single effect evaporation desalination process. Renewable Energy 2001;24:91–111.
[98] Wang X, Ng KC. Experimental investigation of an adsorption desalination plant using low-temperature waste heat. Applied Thermal Engineering 2005;25:2780–9.
[99] Zejli D, Benchrifa R, Bennouna A, Bouhelal OK. A solar adsorption desalination device: first simulation results. Desalination 2004;168:127–35.
[100] Alarcón-Padilla D-C, García-Rodríguez L. Application of absorption heat pumps to multi-effect distillation: a case study of solar desalination. Desalination 2007;212:294–302.
[101] García-Rodríguez L, Gómez-Camacho C. Preliminary design and cost analysis of a solar distillation system. Desalination 1999;126:109–14.
[102] García-Rodríguez L, Gómez-Camacho C. Design parameter selection for a distillation system coupled to a solar parabolic trough collector. Desalination 1999;122:195–204.
[103] García-Rodríguez L, Gómez-Camacho C. Exergy analysis of the SOL-14 plant (Plataforma Solar de Almería, Spain). Desalination 2001;137:251–8.
[104] García-Rodríguez L, Palmero-Marrero AI, Gómez-Camacho C. Thermoeconomic optimization of the SOL-14 plant (plataforma solar de Almería, Spain). Desalination 2001;136:219–23.
[105] Alarcón-Padilla DC, García-Rodríguez L, Blanco-Gálvez J. Design recommendations for a multi-effect distillation plant connected to a double-effect absorption heat pump: a solar desalination case study. Desalination 2010;262:11–4.
[106] Milow B, Zarza E. Advanced MED solar desalination plants Configurations, costs, future—seven years of experience at the Plataforma Solar de Almeria (Spain). Desalination 1997;108:51–8.
[107] García-Rodríguez L, Gómez-Camacho C. Thermo-economic analysis of a solar multi-effect distillation plant installed at the Plataforma Solar de Almeria (Spain). Desalination 1999;122:205–14.
[108] García-Rodríguez L, Palmero-Marrero AI, Gómez-Camacho C. Application of direct steam generation into a solar parabolic trough collector to multieffect distillation. Desalination 1999;125:139–45.
[109] Palenzuela P, Zaragoza G, Alarcón-Padilla DC, Guillén E, Ibarra M, Blanco J. Assessment of different configurations for combined parabolic-trough (PT) solar power and desalination plants in arid regions. Energy 2011;36:4950–8.
[110] Sharaf MA, Nafey AS, García-Rodríguez L. Thermo-economic analysis of solar thermal power cycles assisted MED–VC (multi effect distillation–vapor compression) desalination processes. Energy 2011;36:2753–64.
[111] Helal AM, Al-Malek SA. Design of a solar-assisted mechanical vapor compression (MVC) desalination unit for remote areas in the UAE. Desalination 2006;197:273–300.

[112] Nguyen M, Riffat SB, Whitman D. Solar/gas-driven absorption heat-pump systems. Applied Thermal Engineering 1996;16:347–56.
[113] Alarcón-Padilla D-C, García-Rodríguez L, Blanco-Gálvez J. Assessment of an absorption heat pump coupled to a multi-effect distillation unit within AQUASOL project. Desalination 2007;212:303–10.
[114] Alarcón-Padilla D-C, Blanco-Gálvez J, García-Rodríguezz L, Gernjak W, Malato-Rodríguez S. First experimental results of a new hybrid solar/gas multi-effect distillation system: the AQUASOL project. Desalination 2008;220:619–25.
[115] Roca L, Berenguel M, Yebra L, Alarcón DC. Preliminary modeling and control studies in AQUASOL project. Desalination 2008;222:466–73.
[116] Roca L, Guzman JL, Normey-Rico JE, Berenguel M, Yebra L. Robust constrained predictive feedback linearization controller in a solar desalination plant collector field. Control Engineering Practice 2009;17:1076–88.
[117] Roca L, Berenguel M, Yebra L, Alarcón-Padilla DC. Solar field control for desalination plants. Solar Energy 2008;82:772–86.
[118] Gomri R. Energy and exergy analyses of seawater desalination system integrated in a solar heat transformer. Desalination 2009;249:188–96.
[119] Childs WD, Dabiri AE, Al-Hinai HA, Abdullah HA. VARI–RO solar-powered desalting technology. Desalination 1999;125:155–66.
[120] Hasnain SM, Alajlan SA. Coupling of PV-powered RO brackish water desalination plant with solar stills. Desalination 1998;116:57–64.
[121] Alawaji S, Smiai MS, Rafique S, Stafford B. PV-powered water pumping and desalination plant for remote areas in Saudi Arabia. Applied Energy 1995;52:283–9.
[122] Alajlan SA, Smiai MS. Performance and development of PV—plant for water pumping and desalination for remote area in Saudi Arabia. Renewable Energy 1996;8:441–6.
[123] Parida B, Iniyan S, Goic R. A review of solar photovoltaic technologies. Renewable and Sustainable Energy Reviews 2011;15:1625–36.
[124] Mohamed ES, Papadakis G, Mathioulakis E, Belessiotis V. A direct coupled photovoltaic seawater reverse osmosis desalination system toward battery based systems—a technical and economical experimental comparative study. Desalination 2008;221:17–22.
[125] Amati V, Zapater CH, Sciubba E, Marcuello JU. Process simulation of a reverse Osmosis desalination plant powered by photovoltaic panels for Kalymnos Island. ASME Conference Proceedings 2008:209–17.
[126] Mohamed ES, Papadakis G. Design, simulation and economic analysis of a stand-alone reverse osmosis desalination unit powered by wind turbines and photovoltaics. Desalination 2004;164:87–97.
[127] Bouguecha S, Hamrouni B, Dhahbi M. Small scale desalination pilots powered by renewable energy sources: case studies. Desalination 2005;183:151–65.
[128] Fiorenza G, Sharma VK, Braccio G. Techno-economic evaluation of a solar powered water desalination plant. Energy Conversion and Management 2003;44:2217–40.
[129] Laborde HM, França KB, Neff H, Lima AMN. Optimization strategy for a small-scale reverse osmosis water desalination system based on solar energy. Desalination 2001;133:1–12.
[130] Tzen E, Theofilloyianakos D, Kologios Z. Autonomous reverse osmosis units driven by RE sources experiences and lessons learned. Desalination 2008;221:29–36.
[131] Thomson M, Infield D. Laboratory demonstration of a photovoltaic-powered seawater reverse-osmosis system without batteries. Desalination 2005;183:105–11.
[132] Helal AM, Al-Malek SA, Al-Katheeri ES. Economic feasibility of alternative designs of a PV–RO desalination unit for remote areas in the United Arab Emirates. Desalination 2008;221:1–16.
[133] Tzen E, Theofilloyianakos D, Sigalas M, Karamanis K. Design and development of a hybrid autonomous system for seawater desalination. Desalination 2004;166:267–74.
[134] Espino T, Peñate B, Piernavieja G, Herold D, Neskakis A. Optimised desalination of seawater by a PV powered reverse osmosis plant for a decentralised coastal water supply. Desalination 2003;156:349–50.
[135] Thomson M, Infield D. A photovoltaic-powered seawater reverse-osmosis system without batteries. Desalination 2003;153:1–8.
[136] Thomson M, Miranda MS, Infield D. A small-scale seawater reverse-osmosis system with excellent energy efficiency over a wide operating range. Desalination 2003;153:229–36.
[137] Herold D, Neskakis A. A small PV-driven reverse osmosis desalination plant on the island of Gran Canaria. Desalination 2001;137:285–92.
[138] Al-Alawi A, M Al-Alawi S, M Islam S. Predictive control of an integrated PV-diesel water and power supply system using an artificial neural network. Renewable Energy 2007;32:1426–39.
[139] Kershman SA, Rheinländer J, Neumann T, Goebel O. Hybrid wind/PV and conventional power for desalination in Libya—GECOL's facility for medium and small scale research at Ras Ejder. Desalination 2005;183:1–12.
[140] Nafey AS, Sharaf MA. Combined solar organic Rankine cycle with reverse osmosis desalination process: energy, exergy, and cost evaluations. Renewable Energy 2010;35:2571–80.
[141] Kosmadakis G, Manolakos D, Kyritsis S, Papadakis G. Design of a two stage organic Rankine cycle system for reverse osmosis desalination supplied from a steady thermal source. Desalination 2010;250:323–8.
[142] Kosmadakis G, Manolakos D, Kyritsis S, Papadakis G. Economic assessment of a two-stage solar organic Rankine cycle for reverse osmosis desalination. Renewable Energy 2009;34:1579–86.
[143] Manolakos D, Kosmadakis G, Kyritsis S, Papadakis G. On site experimental evaluation of a low-temperature solar organic Rankine cycle system for RO desalination. Solar Energy 2008.
[144] Kosmadakis G, Manolakos D, Papadakis G. Parametric theoretical study of a two-stage solar organic Rankine cycle for RO desalination. Renewable Energy 2010;35:989–96.
[145] Manolakos D, Papadakis G, Mohamed ES, Kyritsis S, Bouzianas K. Design of an autonomous low-temperature solar Rankine cycle system for reverse osmosis desalination. Desalination 2005;183:73–80.
[146] Kosmadakis G, Manolakos D, Kyritsis S, Papadakis G. Comparative thermodynamic study of refrigerants to select the best for use in the high-temperature stage of a two-stage organic Rankine cycle for RO desalination. Desalination 2009;243:74–94.
[147] Fritzmann C, Löwenberg J, Wintgens T, Melin T. State-of-the-art of reverse osmosis desalination. Desalination 2007;216:1–76.
[148] Delgado-Torres AM, García-Rodríguez L. Preliminary design of seawater and brackish water reverse osmosis desalination systems driven by low-temperature solar organic Rankine cycles (ORC). Energy Conversion and Management 2010;51:2913–20.
[149] Tchanche BF, Lambrinos G, Frangoudakis A, Papadakis G. Exergy analysis of micro-organic Rankine power cycles for a small scale solar driven reverse osmosis desalination system. Applied Energy 2010;87:1295–306.
[150] Delgado-Torres AM, García-Rodríguez L. Comparison of solar technologies for driving a desalination system by means of an organic Rankine cycle. Desalination 2007;216:276–91.
[151] Delgado-Torres AM, García-Rodríguez L. Double cascade organic Rankine cycle for solar-driven reverse osmosis desalination. Desalination 2007;216:306–13.
[152] Delgado-Torres AM, García-Rodríguez L. Preliminary assessment of solar organic Rankine cycles for driving a desalination system. Desalination 2007;216:252–75.
[153] Delgado-Torres AM, García-Rodríguez L, Romero-Ternero VJ. Preliminary design of a solar thermal-powered seawater reverse osmosis system. Desalination 2007;216:292–305.
[154] García-Rodríguez L, Delgado-Torres AM. Solar-powered Rankine cycles for fresh water production. Desalination 2007;212:319–27.
[155] Delgado-Torres AM. Solar thermal heat engines for water pumping: An update. Renewable and Sustainable Energy Reviews 2009;13:462–72.
[156] Delgado-Torres AM, García-Rodríguez L. Status of solar thermal-driven reverse osmosis desalination. Desalination 2007;216:242–51.
[157] Bruno J, Lopezvillada J, Letelier E, Romera S, Coronas A. Modelling and optimisation of solar organic Rankine cycle engines for reverse osmosis desalination. Applied Thermal Engineering 2008;28:2212–26.
[158] Manolakos D, Papadakis G, Kyritsis S, Bouzianas K. Experimental evaluation of an autonomous low-temperature solar Rankine cycle system for reverse osmosis desalination. Desalination 2007;203:366–74.
[159] Kosmadakis G, Manolakos D, Kyritsis S, Papadakis G. Simulation of an autonomous, two-stage solar organic Rankine cycle system for reverse osmosis desalination. Desalination and Water Treatment 2009;1:114–27.
[160] Review of water resources and desalination technologies, by Miller, James Edward, Sandia National Laboratories, Albuquerque, NM 2003.
[161] Xu T, Huang C. Electro-dialysis-based separation technologies: a critical review. AIChE Journal 2008;54:3147–59.
[162] Ortiz JM, Expósito E, Gallud F, García-García V, Montiel V, Aldaz A. Desalination of underground brackish waters using an electro-dialysis system powered directly by photovoltaic energy. Solar Energy Materials and Solar Cells 2008;92:1677–88.
[163] Ortiz JM, Expósito E, Gallud F, García-García V, Montiel V, Aldaz A. Photovoltaic electro-dialysis system for brackish water desalination: modeling of global process. Journal of Membrane Science 2006;274:138–49.
[164] Ishimaru N. Solar photovoltaic desalination of brackish water in remote areas by electro-dialysis. Desalination 1994;98:485–93.
[165] AlMadani HMN. Water desalination by solar powered electro-dialysis process. Renewable Energy 2003;28:1915–24.
[166] Kuroda O, Takahashi S, Kubota S, Kikuchi K, Eguchi Y, Ikenaga Y, et al. An electro-dialysis sea water desalination system powered by photovoltaic cells. Desalination 1987;67:33–41.
[167] Al-Karaghouli A, Renne D, Kazmerski LL. Technical and economic assessment of photovoltaic-driven desalination systems. Renewable Energy 2010;35:323–8.
[168] Sadrzadeh M, Mohammadi T. Treatment of sea water using electro-dialysis: Current efficiency evaluation. Desalination 2009;249:279–85.
[169] Sadrzadeh M, Mohammadi T. Sea water desalination using electro-dialysis. Desalination 2008;221:440–7.
[170] Al-Kharabsheh S, Goswami DY. Theoretical analysis of a water desalination system using low grade solar heat. Journal of Solar Energy Engineering 2004;126:774–80.
[171] Al-Kharabsheh S, Goswami DY. Experimental study of an innovative solar water desalination system utilizing a passive vacuum technique. Solar Energy 2003;75:395–401.
[172] Miyatake O. Comparative study of flash evaporation rates. Desalination 1994;96:163–71.
[173] Abutayeh M, Goswami DY. Passive vacuum solar flash desalination. AIChE Journal 2009;56:1196–203.
[174] Abutayeh M, Goswami DY. Solar flash desalination under hydrostatically sustained vacuum. Journal of Solar Energy Engineering 2009;131:031016–7.

[175] Gude VG, Nirmalakhandan N. Desalination using low-grade heat sources. Journal of Energy Engineering 2008;134:95–101.
[176] Gude VG, Nirmalakhandan N. Desalination at low temperatures and low pressures. Desalination 2009;244:239–47.
[177] Ayhan T, Al Madani H. Feasibilty study of renewable energy powered seawater desalination technology using natural vacuum technique. Renewable Energy 2010;35:506–14.
[178] Gude VG, Nirmalakhandan N. Sustainable desalination using solar energy. Energy Conversion and Management 2010;51:2245–51.
[179] Al-Kharabsheh S, YogiˆGoswami D. Analysis of an innovative water desalination system using low-grade solar heat. Desalination 2003;156: 323–32.
[180] Abutayeh M, Goswami DY. Experimental simulation of solar flash desalination. Journal of Solar Energy Engineering 2010;132:041015–7.
[181] Tripathi R, Tiwari GN. Effect of water depth on internal heat and mass transfer for active solar distillation. Desalination 2005;173:187–200.
[182] Singh HN, Tiwari GN. Monthly performance of passive and active solar stills for different Indian climatic conditions. Desalination 2004;168:145–50.
[183] Kumar S, Tiwari GN. Performance evaluation of an active solar distillation system. Energy 1996;21:805–8.
[184] Lawrence SA, Tiwari GN. Theoretical evaluation of solar distillation under natural circulation with heat exchanger. Energy Conversion and Management 1990;30:205–13.
[185] Tiwari GN, Kumar S, Sharma PB, Emran Khan M. Instantaneous thermal efficiency of an active solar still. Applied Thermal Engineering 1996;16: 189–92.
[186] Yadav YP, Prasad AS. Performance analysis of a high temperature solar distillation system. Energy Conversion and Management 1995;36:365–74.
[187] Badran OO, Al-Tahaineh HA. The effect of coupling a flat-plate collector on the solar still productivity. Desalination 2005;183:137–42.
[188] Fath HES, Elsherbiny SM. Effect of adding a passive condenser on solar still performance. Energy Conversion and Management 1993;34:63–72.
[189] Tay JH, Low SC, Jeyaseelan S. Vacuum desalination for water purification using waste heat. Desalination 1996;106:131–5.
[190] Low SC, Tay PJH. Vacuum desalination using waste heat from a steam turbine. Desalination 1991;81:321–31.
[191] Mink G, Aboabboud MM, Karmazsin É. Air-blown solar still with heat recycling. Solar Energy 1998;62:309–17.
[192] Schwarzer K, Vieira da Silva E, Hoffschmidt B, Schwarzer T. A new solar desalination system with heat recovery for decentralised drinking water production. Desalination 2009;248:204–11.
[193] Fernández J, Chargoy N. Multi-stage indirectly heated solar still. Solar Energy 1990;44:215–23.
[194] Kumar S, Tiwari GN. Optimization of design parameters for multi-effect active distillation systems using the Runge–Kutta method. Desalination 1999;121:87–96.
[195] Tanaka H, Nakatake Y, Tanaka M. Indoor experiments of the vertical multiple-effect diffusion-type solar still coupled with a heat-pipe solar collector. Desalination 2005;177:291–302.
[196] El-Sebaii AA, Al-Ghamdi AA, Al-Hazmi FS, Faidah AS. Thermal performance of a single basin solar still with PCM as a storage medium. Applied Energy 2009;86:1187–95.
[197] Onyegegbu SO. Nocturnal distillation in basin-type solar stills. Applied Energy 1986;24:29–42.
[198] Velmurugan V, Srithar K. Solar stills integrated with a mini solar pond—analytical simulation and experimental validation. Desalination 2007;216:232–41.
[199] Velmurugan V, Mandlin J, Stalin B, Srithar K. Augmentation of saline streams in solar stills integrating with a mini solar pond. Desalination 2009;249:143–9.
[200] Kumar S, Tiwari A. An experimental study of hybrid photovoltaic thermal (PV/T)active solar still. International Journal of Energy Research 2008;32: 847–58.
[201] Hidouri K, Ben Slama R, Gabsi S. Hybrid solar still by heat pump compression. Desalination 2010;250:444–9.
[202] Sampathkumar K, Arjunan TV, Pitchandi P, Senthilkumar P. Active solar distillation—a detailed review. Renewable and Sustainable Energy Reviews 2010;14:1503–26.
[203] Dunkle RV, CSIRO, International heat transfer conference 1961–1962: Boulder C and W Solar water distillation: the roof type still and a multiple effect diffusion still. [Melbourne:: C.S.I.R.O; 1961.
[204] Parekh S, Farid M, Selman J, Alhallaj S. Solar desalination with a humidification–dehumidification technique—a comprehensive technical review. Desalination 2004;160:167–86.
[205] Narayan GP, Sharqawy MH, Summers EK, Lienhard JH, Zubair SM, Antar MA. The potential of solar-driven humidification–dehumidification desalination for small-scale decentralized water production. Renewable and Sustainable Energy Reviews 2010;14:1187–201.
[206] Hisham E. Design and analysis of humidification dehumidification desalination process. Desalination 2005;183:341–52.
[207] Müller-Holst H, Engelhardt M, Herve M, Schölkopf W. Solar thermal seawater desalination systems for decentralised use. Renewable Energy 1998;14:311–8.
[208] Hou S, Zhang H. A hybrid solar desalination process of the multi-effect humidification dehumidification and basin-type unit. Desalination 2008;220:552–7.
[209] Mistry KH, Lienhard V JH, Zubair SM. Effect of entropy generation on the performance of humidification–dehumidification desalination cycles. International Journal of Thermal Sciences 2010;49:1837–47.
[210] Yamall C, Solmus I. A solar desalination system using humidification–dehumidification process: experimental study and comparison with the theoretical results. Desalination 2008;220:538–51.
[211] Abdel Dayem AM, Fatouh M. Experimental and numerical investigation of humidification/dehumidification solar water desalination systems. Desalination 2009;247:594–609.
[212] Amer EH, Kotb H, Mostafa GH, El-Ghalban AR. Theoretical and experimental investigation of humidification–dehumidification desalination unit. Desalination 2009;249:949–59.
[213] Soufari SM, Zamen M, Amidpour M. Performance optimization of the humidification–dehumidification desalination process using mathematical programming. Desalination 2009;237:305–17.
[214] Zhani K, Ben Bacha H. Experimental investigation of a new solar desalination prototype using the humidification dehumidification principle. Renewable Energy 2010;35:2610–7.
[215] Rommel M. Solar thermally driven desalination systems with corrosion-free collectors. Renewable Energy 1998;14:275–80.
[216] Marmouch H, Orfi J, Nasrallah SB. Effect of a cooling tower on a solar desalination system. Desalination 2009;238:281–9.
[217] Hou S, Ye S, Zhang H. Performance optimization of solar humidification–dehumidification desalination process using Pinch technology. Desalination 2005;183:143–9.
[218] Hou S. Two-stage solar multi-effect humidification dehumidification desalination process plotted from pinch analysis. Desalination 2008;222:572–8.
[219] Orfi J, Laplante M, Marmouch H, Galanis N, Benhamou B, Nasrallah SB, et al. Experimental and theoretical study of a humidification–dehumidification water desalination system using solar energy. Desalination 2004;168: 151–9.
[220] Orfi J, Galanis N, Laplante M. Air humidification–dehumidification for a water desalination system using solar energy. Desalination 2007;203: 471–81.
[221] Alhazmy MM. Minimum work requirement for water production in humidification–dehumidification desalination cycle. Desalination 2007;214:102–11.
[222] Eslamimanesh A, Hatamipour MS. Economical study of a small-scale direct contact humidification–dehumidification desalination plant. Desalination 2010;250:203–7.
[223] Eslamimanesh A, Hatamipour MS. Mathematical modeling of a direct contact humidification–dehumidification desalination process. Desalination 2009;237:296–304.
[224] Zamen M, Amidpour M, Soufari SM. Cost optimization of a solar humidification–dehumidification desalination unit using mathematical programming. Desalination 2009;239:92–9.
[225] Fath HES, Ghazy A. Solar desalination using humidification–dehumidification technology. Desalination 2002;142:119–33.
[226] Cipollina A, Micale G Coupling sustainable energy with membrane distillation processes for seawater desalination. In: Nuclear & Renewable Energy Conference (INREC), 2010 1st International, 2010, p. 1–6.
[227] Al-Obaidani S, Curcio E, Macedonio F, Di Profio G, Al-Hinai H, Drioli E. Potential of membrane distillation in seawater desalination: thermal efficiency, sensitivity study and cost estimation. Journal of Membrane Science 2008;323:85–98.
[228] Alklaibi AM, Lior N. Membrane-distillation desalination: status and potential. Desalination 2005;171:111–31.
[229] Cath TY, Adams VD, Childress AE. Experimental study of desalination using direct contact membrane distillation: a new approach to flux enhancement. Journal of Membrane Science 2004;228:5–16.
[230] Meindersma GW, Guijt CM, de Haan AB. Desalination and water recycling by air gap membrane distillation. Desalination 2006;187:291–301.
[231] Mericq J-P, Laborie S, Cabassud C. Evaluation of systems coupling vacuum membrane distillation and solar energy for seawater desalination. Chemical Engineering Journal 2011;166:596–606.
[232] Banat F, Jwaied N, Rommel M, Koschikowski J, Wieghaus M. Performance evaluation of the large SMADES autonomous desalination solar-driven membrane distillation plant in Aqaba, Jordan. Desalination 2007;217: 17–28.
[233] Banat F, Jwaied N. Economic evaluation of desalination by small-scale autonomous solar-powered membrane distillation units. Desalination 2008;220:566–73.
[234] Zwijnenberg HJ, Koops GH, Wessling M. Solar driven membrane pervaporation for desalination processes. Journal of Membrane Science 2005;250: 235–46.
[235] Chen T-C, Ho C-D. Immediate assisted solar direct contact membrane distillation in saline water desalination. Journal of Membrane Science 2010;358:122–30.
[236] Dotremont C. Seawater desalination with memstill technology —a sustainable solution for the industry. Water Practice and Technology 2010;5:1–7.
[237] Minton Paul, E. Handbook of Evaporation Technology 1986.
[238] Gastli A, Charabi Y, Zekri S. GIS-based assessment of combined CSP electric power and seawater desalination plant for Duqum–Oman. Renewable and Sustainable Energy Reviews 2010;14:821–7.
[239] Hamed OA, Eisa EI, Abdalla WE. Overview of solar desalination. Desalination 1993;93:563–79.

[240] Papapetrou M, Wieghaus M, Biercamp C Roadmap for the development of desalination powered by renewable energy-promotion for renewable energy for water production through Desalination. Hrsg.: Fraunhofer ISE, Freiburg/Brsg.; 2010.
[241] Zhou X, Xiao B, Liu W, Guo X, Yang J, Fan J. Comparison of classical solar chimney power system and combined solar chimney system for power generation and seawater desalination. Desalination 2010;250:249–56.
[242] Semiat R. Energy issues in desalination processes. Environmental Science & Technology 2008;42:8193–201.
[243] Cerci Y. The minimum work requirement for distillation processes. Exergy, An International Journal 2002;2:15–23.
[244] F-Chart Software: 〈www.fchart.com〉.
[245] Stoughton RW, Lietzke MH. Thermodynamic properties of sea salt solutions. Journal of Chemical & Engineering Data 1967;12:101–4.
[246] Sharqawy M, Lienhard V JH, Zubair SM. Thermophysical peoperties of seawater: a review of existing correlations and data. Desalination and Water Treatment 2010;16:354–80.
[247] Elimelech M, Phillip WA. The future of seawater desalination: energy, technology, and the environment. Science 2011;333:712–7.
[248] Liu Z, Bai H, Lee J, Sun DD. A low-energy forward osmosis process to produce drinking water. Energy & Environmental Science 2011;4:2582.
[249] McGinnis RL, Elimelech M. Energy requirements of ammonia-carbon dioxide forward osmosis desalination. Desalination 2007;207:370–82.
[250] Spiegler KS, Laird ADK. Principles of desalination. 2nd ed.Academic Press Inc; 1980.
[251] Spiegler KS, El-Sayed YM. The energetics of desalination processes. Desalination 2001;134:109–28.
[252] DODGE BF, ESHAYA AM. Thermodynamics of some desalting processes. In: Saline water conversion, 27. American Chemical Society; 1960 7–20.
[253] Narayan GP, Sharqawy MH, Lienhard V JH, Zubair SM. Thermodynamic analysis of humidification–dehumidification desalination cycles. Desalination and Water Treatment 2010;16:339–53.
[254] Suárez F, Tyler SW, Childress AE. A theoretical study of a direct contact membrane distillation system coupled to a salt-gradient solar pond for terminal lakes reclamation. Water Research 2010;44:4601–15.
[255] Bouzayani N, Galanis N, Orfi J. Thermodynamic analysis of combined electric power generation and water desalination plants. Applied Thermal Engineering 2009;29:624–33.
[256] Koschikowski J, Wieghaus M, Rommel M, Ortin VS, Suarez BP, Betancort Rodríguez JR. Experimental investigations on solar driven stand-alone membrane distillation systems for remote areas. Desalination 2009;248: 125–31.
[257] Fath HES, Elsherbiny SM, Hassan AA, Rommel M, Wieghaus M, Koschikowski J, et al. PV and thermally driven small-scale, stand-alone solar desalination systems with very low maintenance needs. Desalination 2008;225:58–69.
[258] Wade NM. Technical and economic evaluation of distillation and reverse osmosis desalination processes. Desalination 1993;93:343–63.
[259] Abutayeh M Theoretical and experimental simulation of passive vacuum solar flash desalination. University of South Florida, 2010.
[260] Deng R, Xie L, Lin H, Liu J, Han W. Integration of thermal energy and seawater desalination. Energy 2010;35:4368–74.
[261] Manolakos D, Mohamed ES, Karagiannis I, Papadakis G. Technical and economic comparison between PV and RO system and RO-Solar Rankine system. Case study: Thirasia island. Desalination 2008;221:37–46.
[262] Sharma A, Tyagi VV, Chen CR, Buddhi D. Review on thermal energy storage with phase change materials and applications. Renewable and Sustainable Energy Reviews 2009;13:318–45.
[263] Mills D. Advances in solar thermal electricity technology. Solar Energy 2003;76:19–31.
[264] Technology roadmap—concentrating solar power 2010.
[265] Center for International Earth Science Information Network (CIESIN).
[266] Hussain A, Gobaisi DA, El-Nashar AM. Application of solar energy in desalting seawater. In: Goswami DY, Zhao Y, (eds.), Proceedings of ISES World Congress 2007 (vol. I–V), Berlin, Heidelberg: Springer Berlin Heidelberg; 2008, p. 2799–2804.
[267] Baños R, Manzano-Agugliarob F, Montoya FG, Gil C, Alcayde A, Gómez J. Optimization methods applied to renewable and sustainable energy: a review. Renewable and Sustainable Energy Reviews 2011;15:1753–66.
[268] Fernández-García A, Zarza E, Valenzuela L, Pérez M. Parabolic-trough solar collectors and their applications. Renewable and Sustainable Energy Reviews 2010;14:1695–721.
[269] Chen H, Goswami DY, Stefanakos EK. A review of thermodynamic cycles and working fluids for the conversion of low-grade heat. Renewable and Sustainable Energy Reviews 2010;14:3059–67.
[270] Roeb M, Neises M, Monnerie N, Sattler C, Pitz-Paal R. Technologies and trends in solar power and fuels. Energy & Environmental Science 2011;4:2503.
[271] Müller B, Arlt W, Wasserscheid P. A new concept for the global distribution of solar energy: energy carrying compounds. Energy & Environmental Science 2011.
[272] Tapiador FJ. Assessment of renewable energy potential through satellite data and numerical models. Energy & Environmental Science 2009;2:1142.
[273] Papapetrou M, Mohamed ES, Manolakos D, Papadakis G, Subiela VJ, Peñate B. Operating RE/desalination units. In: Micale G, Rizzuti L, Cipollina A, editors. Seawater desalination, Berlin, Heidelberg. Berlin Heidelberg: Springer; 2009. p. 247–72.
[274] Khedr M. Techno-economic investigation of an air humidification–dehumidification desalination process. Chemical Engineering & Technology 1993;16:270–4.
[275] Houcine I, BenAmara M, Guizani A, Maâlej M. Pilot plant testing of a new solar desalination process by a multiple-effect-humidification technique. Desalination 2006;196:105–24.
[276] Chaibi MT, Safi MJ, Hsairi M. Performance analysis of a solar desalting unit in south tunisia. Desalination 1991;82:187–96.
[277] MüLler-Holst H. Solar thermal desalination using the multiple effect humidification (MEH) method. Solar desalination for the 21st Century Dordrecht, Springer Netherlands; p. 215–225.
[278] Carvalho PCM, Riffel DB, Freire C. Montenegro FFD. The Brazilian experience with a photovoltaic powered reverse osmosis plant. Progress in Photovoltaics: Research and Applications 2004;12:373–85.
[279] Keeper BG, Hembree RD, Schrack FC. Optimized matching of solar photovoltaic power with reverse osmosis desalination. Desalination 1985;54:89–103.
[280] Herold D, Horstmann V, Neskakis A, Plettner-Marliani J, Piernavieja G, Calero R. Small scale photovoltaic desalination for rural water supply—demonstration plant in Gran Canaria. Renewable Energy May;14:293–298.
[281] Tzen E, Perrakis K, Baltas P. Design of a stand alone PV—desalination system for rural areas. Desalination 1998;119:327–33.
[282] Madani AA. Economics of desalination for three plant sizes. Desalination 1990;78:187–200.
[283] Delyannis EE, Delyannis A. Economics of solar stills. Desalination 1985;52:167–76.
[284] Kabeel AE, Hamed AM, El-Agouz SA. Cost analysis of different solar still configurations. Energy 2010;35:2901–8.
[285] Walton J, Huanmin L, Turner C, Solis S, and Hein H. Solar and waste heat desalination by membrane distillation; U.S. Department of the Interior Bureau of Reclamation, Desalination and Water Purification Research and Development Program Report 81, Apr. 2004.
[286] Koschikowski J, Wieghaus M, Rommel M, Ortin VS, Suarez BP, Betancort Rodríguez JR. Experimental investigations on solar driven stand-alone membrane distillation systems for remote areas. Desalination 2009;248:125–31.
[287] Banat F, Jwaied N, Rommel M, Koschikowski J, Wieghaus M. Desalination by a 'compact SMADES' autonomous solar powered membrane distillation unit. Desalination 2007;217:29–37.
[288] Banat F, Jumah R, Garaibeh M. Exploitation of solar energy collected by solar stills for desalination by membrane distillation. Renewable Energy 2002;25:293–305.
[289] Chang H, Wang GB, Chen YH, Li CC, Chang CL. Modeling and optimization of a solar driven membrane distillation desalination system. Renewable Energy 2010;35:2714–22.
[290] BlancoGálvez J, García-Rodríguez L, Martín-Mateos I. Seawater desalination by an innovative solar-powered membrane distillation system: the MEDESOL project. Desalination 2009;246:567–76.
[291] Li CN, Besarati S, Goswami Y, Stefanakos E, Chen HJ. Reverse osmosis desalination driven by low temperature supercritical organic Rankine cycle, Applied Energy, http://dx.doi.org/10.1016/j.apenergy.2012.06.028, in press.
[292] Li CN, Goswami Y, Shapiro A, Stefanakos E. A new combined power and desalination system driven by low grade heat for concentrated brine. Energy 2012;46:582–95.